Research Paper

Multifaceted investigation underlies diverse mechanisms contributing to the downregulation of Hedgehog pathway-associated genes *INTU* and *IFT88* in lung adenocarcinoma and uterine corpus endometrial carcinoma

Ho Yin Edwin Chan[1] and Zhefan Stephen Chen[1]

[1]School of Life Sciences, Faculty of Science, The Chinese University of Hong Kong, Hong Kong SAR, China

Correspondence to: Ho Yin Edwin Chan, Zhefan Stephen Chen; **email:** hyechan@cuhk.edu.hk, b140892@cuhk.edu.hk
Keywords: DNA methylation, genomic alteration, Hedgehog pathway, non-coding RNAs, transcription factor
Received: June 1, 2022 **Accepted:** August 25, 2022 **Published:** September 7, 2022

ABSTRACT

Hedgehog (Hh) signaling primarily functions in the control of mammalian embryonic development but also has roles in cancer. The Hh activation depends on ciliogenesis, a cellular process that describes outgrowth of the primary cilium from cell membrane. Ciliogenesis initiation requires a set of proteins known as planar cell polarity (PCP) effectors. Inturned (INTU) is a PCP effector that reportedly functions synergistically with Hh signaling in basal cell carcinoma, suggesting that INTU has an oncogenic role. In this study, we carried out a pan-cancer investigation on the prognostic significance of *INTU* in different types of cancer. We demonstrated that *INTU* downregulation correlated with reduced survival probabilities in lung adenocarcinoma (LUAD) and uterine corpus endometrial carcinoma (UCEC) patients. Similar expression patterns and prognostic values were identified for *intraflagellar transport 88* (*IFT88*), another Hh pathway-associated gene. We elucidated multiple mechanisms at transcriptional, post-transcriptional and translational levels that involved transcription factor 4 and non-coding RNAs-associated regulatory networks contributing to the reduction of *INTU* and *IFT88* levels in LUAD and UCEC samples. Taken together, this study demonstrates the prognostic significance of the Hh-related genes *INTU* and *IFT88* in LUAD and UCEC and further delineates multifaceted mechanisms leading to *INTU* and *IFT88* downregulation in tumor samples.

INTRODUCTION

The Hedgehog (Hh) pathway is an evolutionarily conserved signaling axis essential for the regulation of diverse fundamental biological processes, including embryogenesis and tissue homeostasis [1]. Four major components, including Hh ligands, the Patched (PTCH) receptor, the Smoothened (SMO) intermediator and the zinc finger-containing Glioblastoma (GLI) transcription factor, are crucial for mediating signal transduction from the cell membrane to the nucleus. In the absence of Hh ligands, SMO function is inactivated by the PTCH receptor. GLI is converted to the repressor form, which blocks gene transcription. Upon the binding of Hh ligands to the PTCH receptor, SMO inhibition is relieved, leading to the nuclear accumulation of GLI and subsequent activation of Hh target genes [2].

The Hh pathway is crucial for mammalian embryonic development. Activation of the Hh pathway depends on the presence of a specialized cellular organelle known as the primary cilium, where the active SMO protein resides to promote the nuclear translocation of GLI proteins [3]. Normal ciliogenesis relies on a group of planar cell polarity (PCP) effector proteins, including

the fuzzy planar cell polarity protein (FUZ), the inturned planar cell polarity protein (INTU) and the WD repeat containing planar cell polarity effector (WDPCP) [4, 5]. The intraflagellar transport (IFT) machinery governs the designated distribution of cargo proteins alongside the ciliary axoneme in support of ciliogenesis and activation of Hh signaling [6]. IFT-A and IFT-B are two subsets of protein complexes necessary for controlling retrograde and anterograde trafficking of cargo proteins [7]. The PCP effectors are indispensable for the initial ciliary recruitment and subsequent transport of IFT-A proteins. In mammalian embryos lacking these essential PCP effector genes, both IFT-A and IFT-B trafficking are impaired. In turn, failure of Hh signaling occurs due to ciliogenesis defects, and this leads to severe developmental retardation and early embryonic mortality [4, 5, 8].

Recently, emerging evidence has emphasized the involvement of the Hh pathway in human age-related disorders and cancers [9]. Oncogenic functions have been assigned to all PCP effectors [10–12]. Interestingly, INTU function was found to be related to the Hh pathway during carcinogenesis [12]. In basal cell carcinoma (BCC), *INTU* expression was aberrantly upregulated, accompanied by the induction of Hh signaling. The disruption of *INTU* in a BCC mouse model ameliorated tumorigenesis, and Hh activation was simultaneously suppressed [12]. Moreover, INTU was found to be functionally upstream of GLI transcription factors. Depletion of *INTU* attenuated the expression of *GLI1* and blocked activation of Hh. However, overexpression of a constitutively activated GLI protein was capable of restoring Hh pathway activity in *INTU*-deficient cells [12]. These findings therefore suggest that INTU plays an important oncogenic function in BCC and highlight a synergistic mechanism involving INTU and Hh signaling in carcinogenesis. To date, the involvement of INTU in other cancer types remains elusive.

In this study, we carried out a comprehensive examination on the prognostic values of *INTU* in 21 different types of cancer. We found that the downregulation of *INTU* was associated with poor prognosis in lung adenocarcinoma (LUAD) and uterine corpus endometrial carcinoma (UCEC) patients. A group of Hh pathway-related genes, including *INTU* and *intraflagellar transport 88* (*IFT88*), were enriched in LUAD and UCEC tumor samples. We further demonstrated positive correlations between *INTU* and *IFT88* levels in both LUAD and UCEC samples, and identified multiple mechanisms spanning transcriptional, post-transcriptional and translational aspects that contribute to *INTU* and *IFT88* down-regulation in LUAD and UCEC samples. Taken together, we investigated at multifaceted levels the underlying mechanisms leading to the downregulation of Hh-related genes *INTU* and *IFT88*, and further highlighted the prognostic significance of this downregulation in LUAD and UCEC patients.

RESULTS

Investigations on the prognostic values of *INTU* in multiple cancer types

The Kaplan-Meier plotter was initially used to assess the prognostic significance of *INTU* expression in 21 types of cancer. We found that *INTU* expression was significantly associated with the overall survival (OS) probabilities in patients with nine different cancer types. In liver hepatocellular carcinoma (LIHC) and lung squamous cell carcinoma (LUSC), patients with an increased level of *INTU* had poor OS probabilities. However, in the remaining cancer types, including esophageal adenocarcinoma (EAC), esophageal squamous cell carcinoma (ESCC), kidney renal papillary cell carcinoma (KIRP), LUAD, pancreatic ductal adenocarcinoma (PDAC), sarcoma (SARC) and UCEC, reduced levels of *INTU* were correlated with decreased OS probabilities in patients (Figure 1).

Hh pathway-related genes were enriched in LUAD and UCEC tumor samples

We next sought to evaluate the expression of *INTU* in tumor samples from different cancer types. The expression of *INTU* in tumor samples from The Cancer Genome Atlas (TCGA) were compared with that from normal samples from TCGA and The Genotype-Tissue Expression project (GTEx). The results showed that the *INTU* transcription level was significantly down-regulated in LUAD, LUSC and UCEC samples, whereas in esophageal carcinoma, KIRP, LIHC and SARC, no significant change of *INTU* expression between tumor and normal samples was detected (Figure 2A and Supplementary Figure 1A). No significant changes in the expression of housekeeping genes, including *beta-actin* (*ACTB*), *beta-2-microglobulin* (*B2M*) and *ubiquitin C* (*UBC*), were detected in LUAD and UCEC tumor samples when compared to their respective normal samples (Supplementary Figure 1B). In line with our prognostic analysis, the lower levels of *INTU* in LUAD and UCEC tumor samples (Figure 2A) coincided with poor OS probabilities in cancer patients (Figure 1). We thus decided to focus on LUAD and UCEC in our subsequent studies.

The Gene Expression Profiling Interactive Analysis 2 (GEPIA2) database was used to select the top 100 genes

with similar expression patterns as *INTU* from LUAD and UCEC tumor samples (Supplementary Table 1). We then performed gene enrichment analysis to investigate whether certain enriched Gene Ontology (GO) terms and Reactome pathways could be identified from the LUAD and UCEC gene sets. We found that in LUAD, genes were enriched in cilium-associated biological processes, including cilium morphogenesis, assembly

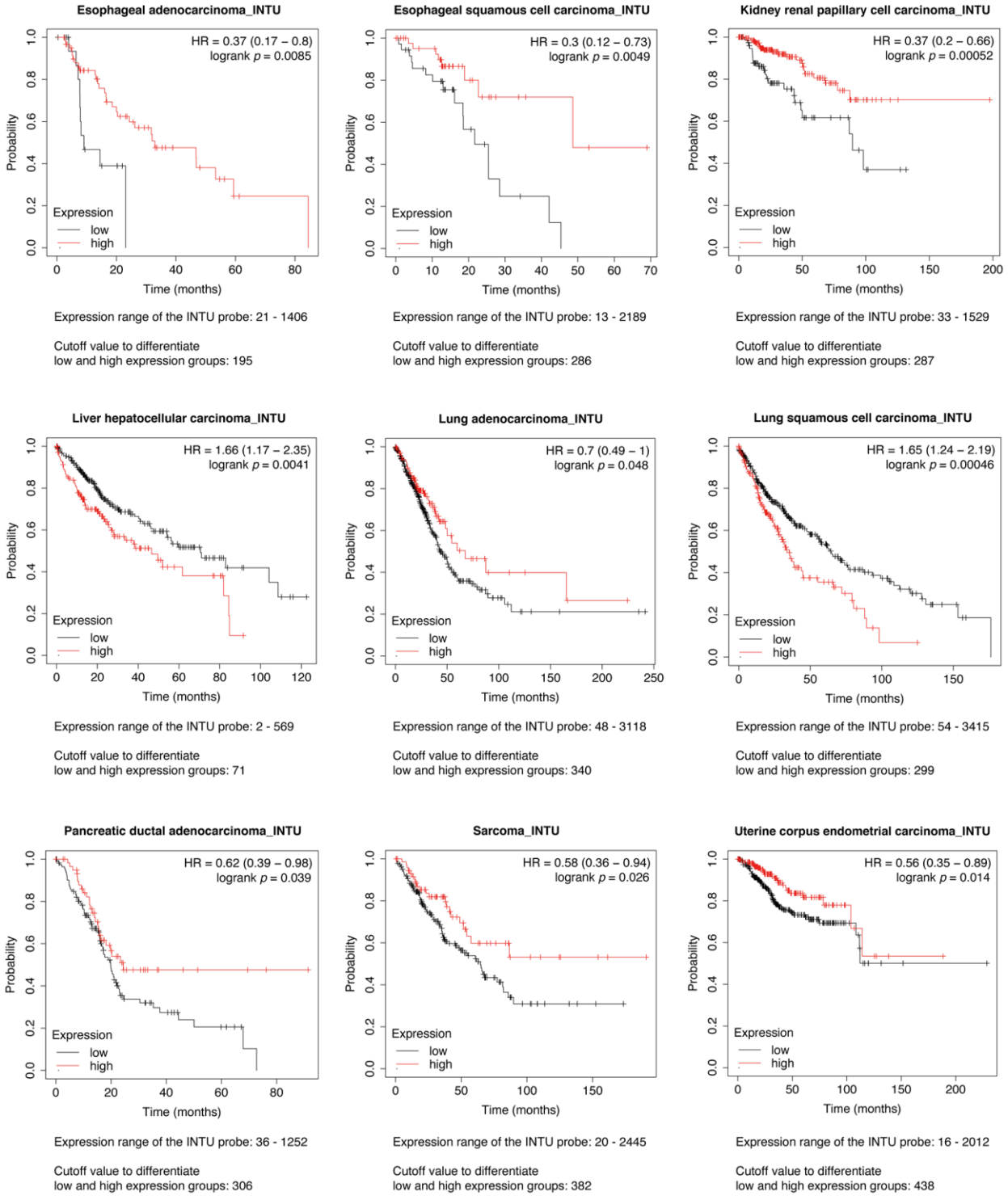

Figure 1. Evaluation of the prognostic significance of *INTU* mRNA level in different cancer types. Pan-cancer survival analysis was carried out to determine the relationship between *INTU* mRNA level and OS probabilities in 21 different types of cancer. Decreased *INTU* expression was found associated with poor prognosis in EAC, ESCC, KIRP, LUAD, PDAC, SARC and UCEC patients, whilst high level of *INTU* correlated with poor prognosis in LIHC and LUSC patients.

and movement. The most enriched subcellular localization pattern was found in association with ciliary compartments. Meanwhile, two Reactome pathways, "Anchoring of the basal body to the plasma membrane" and "Hedgehog 'off' state," were highlighted (Figure 2B). Similar enriched biological

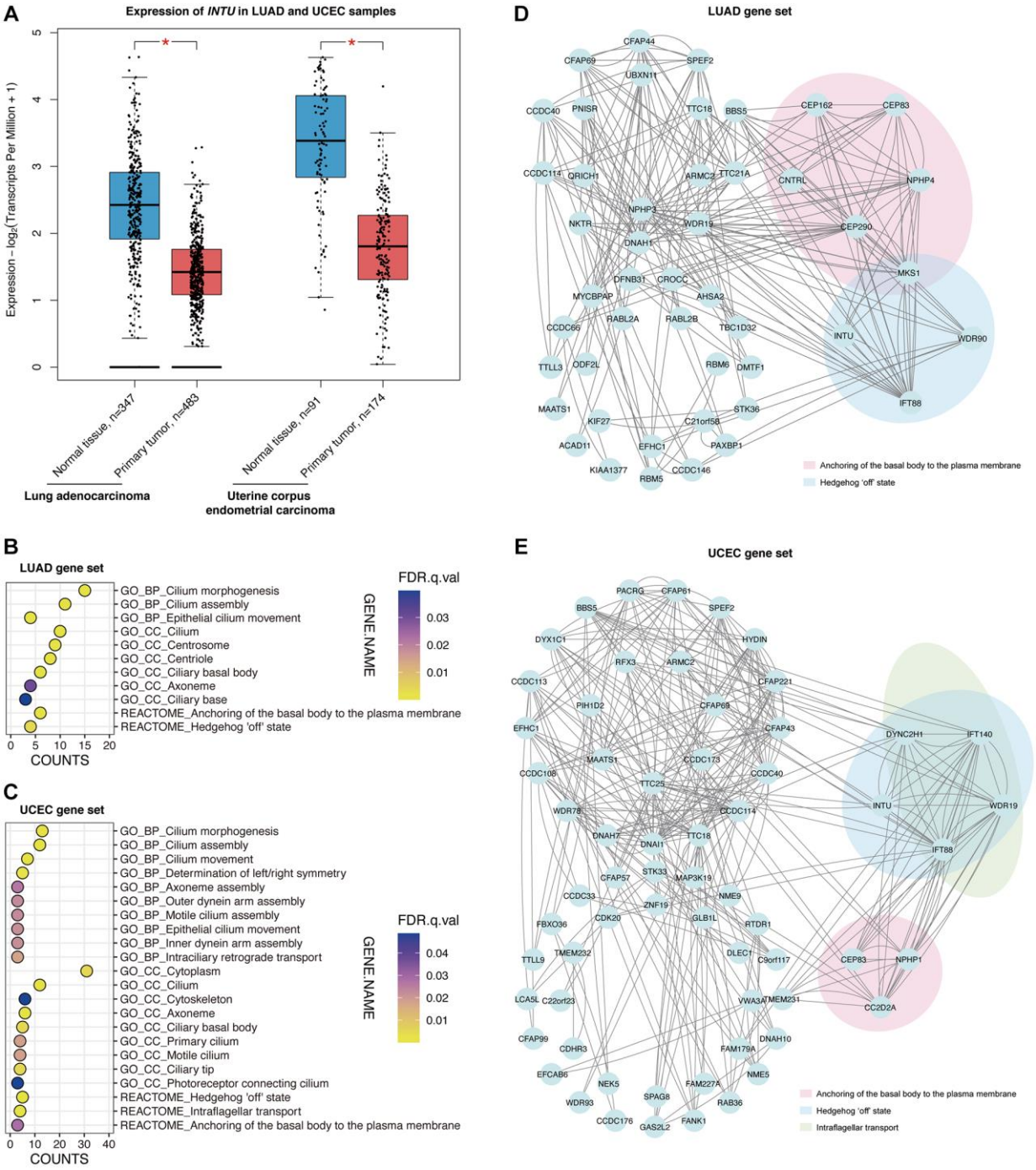

Figure 2. The Hh pathway-associated genes were enriched in LUAD and UCEC tumor samples. (**A**) The expression of *INTU* was significantly downregulated in LUAD and UCEC tumor samples. * denotes $p < 0.05$. (**B**) The GO and Reactome enrichment analysis on the top 100 genes that showed similar expression pattern as *INTU* from LUAD tumor samples. BP indicates biological process, and CC indicates cellular compartment. (**C**) The GO and Reactome enrichment analysis on the top 100 genes that showed similar expression pattern as *INTU* from UCEC tumor samples. (**D**) Construction of the PPI network using genes that showed similar expression pattern as *INTU* in LUAD tumor samples. Two enriched Reactome pathways "Anchoring of the basal body to the plasma membrane" and "Hedgehog 'off' state" were highlighted. (**E**) Construction of the PPI network using genes that showed similar expression pattern as *INTU* in UCEC tumor samples. Three enriched Reactome pathways "Anchoring of the basal body to the plasma membrane", "Hedgehog 'off' state" and "Intraflagellar transport" were highlighted.

processes and cellular compartment terms were identified from the UCEC gene set, where genes were found enriched in three Reactome pathways, including the "Hedgehog 'off' state", "Intraflagellar transport" and "Anchoring of the basal body to the plasma membrane" pathways (Figure 2C).

Protein–protein interaction networks were subsequently constructed. In the LUAD gene set, the centrosomal genes *centrosomal protein 83* (*CEP83*), *centrosomal protein 162* (*CEP162*), *centrosomal protein 290* (*CEP290*), *centriolin* (*CNTRL*), *nephrocystin 4* (*NPHP4*) and *MKS transition zone complex subunit 1* (*MKS1*) were associated with the "Anchoring of the basal body to the plasma membrane" pathway, while *INTU*, *IFT88*, *MKS1* and *WD repeat domain 90* (*WDR90*) were involved in the "Hedgehog 'off' state" pathway (Figure 2D). In the UCEC gene set, *coiled-coil and C2 domain containing 2A* (*CC2D2A*), *CEP83* and *nephrocystin 1* (*NPHP1*) were found in the "Anchoring of the basal body to the plasma membrane" pathway. The protein transport-associated genes *dynein cytoplasmic 2 heavy chain 1* (*DYNC2H1*), *IFT88*, *intraflagellar transport 140* (*IFT140*) and *WD repeat domain 19* (*WDR19*) were involved in the "Intraflagellar transport" pathway, while *DYNC2H1*, *INTU*, *IFT88*, *IFT140* and *WDR19* were involved in the "Hedgehog 'off' state" pathway (Figure 2E).

IFT88 downregulation was associated with the poor prognosis of LUAD and UCEC patients

Similar to *INTU*, *IFT88* was implicated in the "Hedgehog 'off' state" pathway in both the LUAD and UCEC gene sets (Figure 2D, 2E). In addition, *INTU* expression significantly correlated with the expression of *IFT88* from LUAD and UCEC tumor samples (Figure 3A, 3B). Similar to *INTU* (Figure 1), we found that LUAD and UCEC patients with lowered *IFT88* levels also showed decreased OS probabilities (Figure 3C, 3D). Taken together, these results highlight the significance of the downregulation of the Hh pathway-associated genes *INTU* and *IFT88* in the prognosis of LUAD and UCEC patients. We therefore sought to delineate the underlying mechanisms of *INTU* and *IFT88* downregulation in LUAD and UCEC tumor samples.

The methylation level of *INTU* gene promoter CpG islands was upregulated in LUAD and UCEC tumor samples

DNA methylation is a typical epigenetic modification through which gene expression is modulated [13]. In gene promoter region, CpG islands are regions with densely-accumulated CG dinucleotides, and methylation of CpG islands leads to gene silencing [14]. In each of the *INTU* and *IFT88* gene promoter regions, two putative CpG islands were identified (Figure 3E, 3F). To investigate the association between DNA methylation and *INTU* and *IFT88* gene expression, the LUAD (NCI-H1975) and UCEC (AN3 CA) cell lines were treated with 5-azacytidine, a DNA methyl-transferase inhibitor [15], the *INTU* and *IFT88* levels were subsequently detected. We found that upon treatment of 5-azacytidine, both *INTU* and *IFT88* levels were upregulated in NCI-H1975 and AN3 CA cells, suggesting a negative correlation between DNA methylation and *INTU* and *IFT88* gene expression (Figure 3G–3J). The methylation levels of $INTU^{CpG}$ and $IFT88^{CpG}$ were further examined in LUAD and UCEC tumor samples. We found that the methylation level of $INTU^{CpG}$ was significantly upregulated in both LUAD and UCEC tumor samples (Figure 3K). When compared with normal tissues, no significant change in $IFT88^{CpG}$ methylation levels was detected in LUAD and UCEC tumor samples (Figure 3L). This suggests that hypermethylation of $INTU^{CpG}$ potentially contributes to the reduction of *INTU* levels in LUAD and UCEC samples.

Involvement of the transcriptional factor TCF4 in the modulation of *INTU* and *IFT88* levels

Transcription factors are a set of regulatory proteins that bind to gene promoter DNA sequences and modulate gene transcription [16]. A total of nine communal transcription factors, including core-binding factor subunit beta (CBFB), histone deacetylase 2 (HDAC2), transcription factor jun-D (JUND), serum response factor (SRF), small ubiquitin-like modifier 2 (SUMO2), TATA-box binding protein associated factor 1 (TAF1), TATA box binding protein (TBP), transcription factor 4 (TCF4) and yin yang 1 (YY1), were identified in the *INTU* and *IFT88* gene promoters (Figure 4A). Next, we evaluated the expression of these transcription factors in LUAD and UCEC samples. Among these nine transcription factors, we found that only *TCF4* (Figure 4B) expression was significantly downregulated in both LUAD and UCEC tumor samples (Figure 4C and Supplementary Figure 2). The TCF4 protein level was further found to be significantly reduced in both LUAD (Figure 4D) and UCEC (Figure 4E) samples. More importantly, the expression of *TCF4* was positively correlated with the expression of *INTU* and *IFT88* in LUAD and UCEC samples (Figure 4F, 4G). Similar to *INTU* (Figure 1) and *IFT88* (Figure 3C, 3D), the reduced levels of *TCF4* were associated with decreased OS probabilities in LUAD and UCEC patients (Figure 4H, 4I). Altogether, TCF4 was identified as a putative upstream regulator in controlling the expression of *INTU* and *IFT88* in LUAD and UCEC tumor samples.

We further provided experimental evidence in support of our findings. Chromatin immunoprecipitation was performed to investigate the interaction between TCF4 protein and *INTU* and *IFT88* gene promoters. We found that in both the NCI-H1975 and AN3 CA cells, the binding of TCF4 to *INTU* and *IFT88* gene promoters was detected (Figure 5A, 5B). The transcriptional regulatory function of TCF4 on *INTU* and *IFT88* gene expression was subsequently determined. When endogenous *TCF4* was knocked down in NCI-H1975 and AN3 CA cells, the transcript levels of *INTU* and *IFT88* were downregulated (Figure 5C, 5D). These data

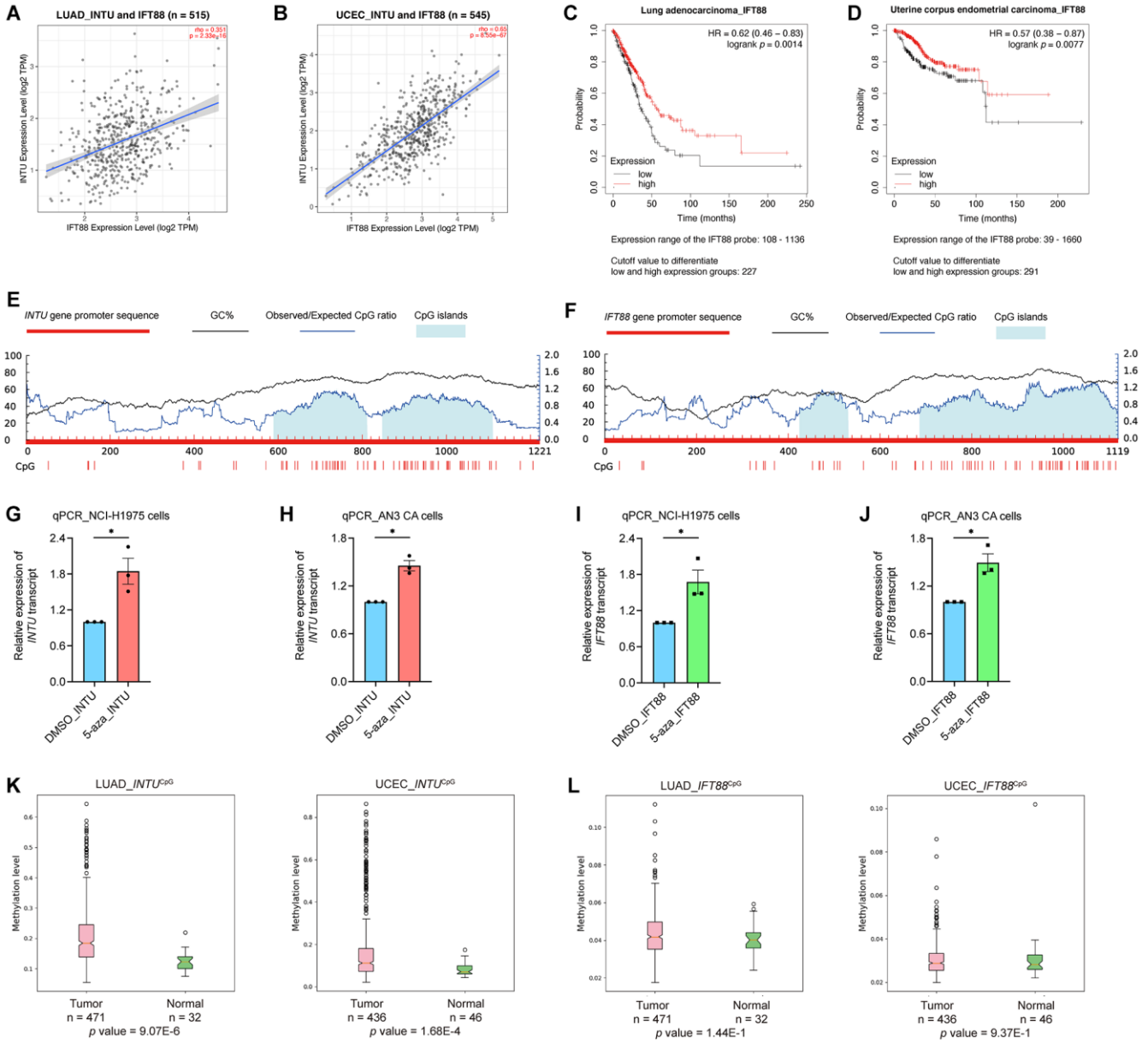

Figure 3. The expression of *IFT88* correlated with *INTU* expression in LUAD and UCEC samples, and hypermethylation of *INTU*^{CpG} was detected in LUAD and UCEC samples. (**A**, **B**) The expression of *IFT88* positively correlated with the expression of *INTU* in LUAD (**A**) and UCEC (**B**) tumor samples. (**C**, **D**) Decreased expression of *IFT88* was found associated with reduced OS probabilities in LUAD (**C**) and UCEC (**D**) patients. (**E**) Two putative CpG islands were identified in *INTU* gene promoter. (**F**) Two CpG islands were predicted in *IFT88* gene promoter. (**G**, **H**) Treatment of 5-azacytidine induced *INTU* expression in NCI-H1975 (**G**) and AN3 CA (**H**) cells. *n* = 3 biological replicates. Each *n* represents an independent preparation of cell RNA samples. Error bars represent S.E.M. Statistical analysis was performed using two-tailed unpaired Student's *t*-test. * denotes $p < 0.05$. (**I**, **J**) Treatment of 5-azacytidine induced *IFT88* expression in NCI-H1975 (**I**) and AN3 CA (**J**) cells. *n* = 3 biological replicates. Each *n* represents an independent preparation of cell RNA samples. Error bars represent S.E.M. Statistical analysis was performed using two-tailed unpaired Student's *t*-test. * denotes $p < 0.05$. (**K**) Hypermethylation of the *INTU*^{CpG} was detected in LUAD and UCEC tumor samples. (**L**) No difference in *IFT88*^{CpG} methylation levels were detected in LUAD and UCEC samples when compared to their respective normal control samples.

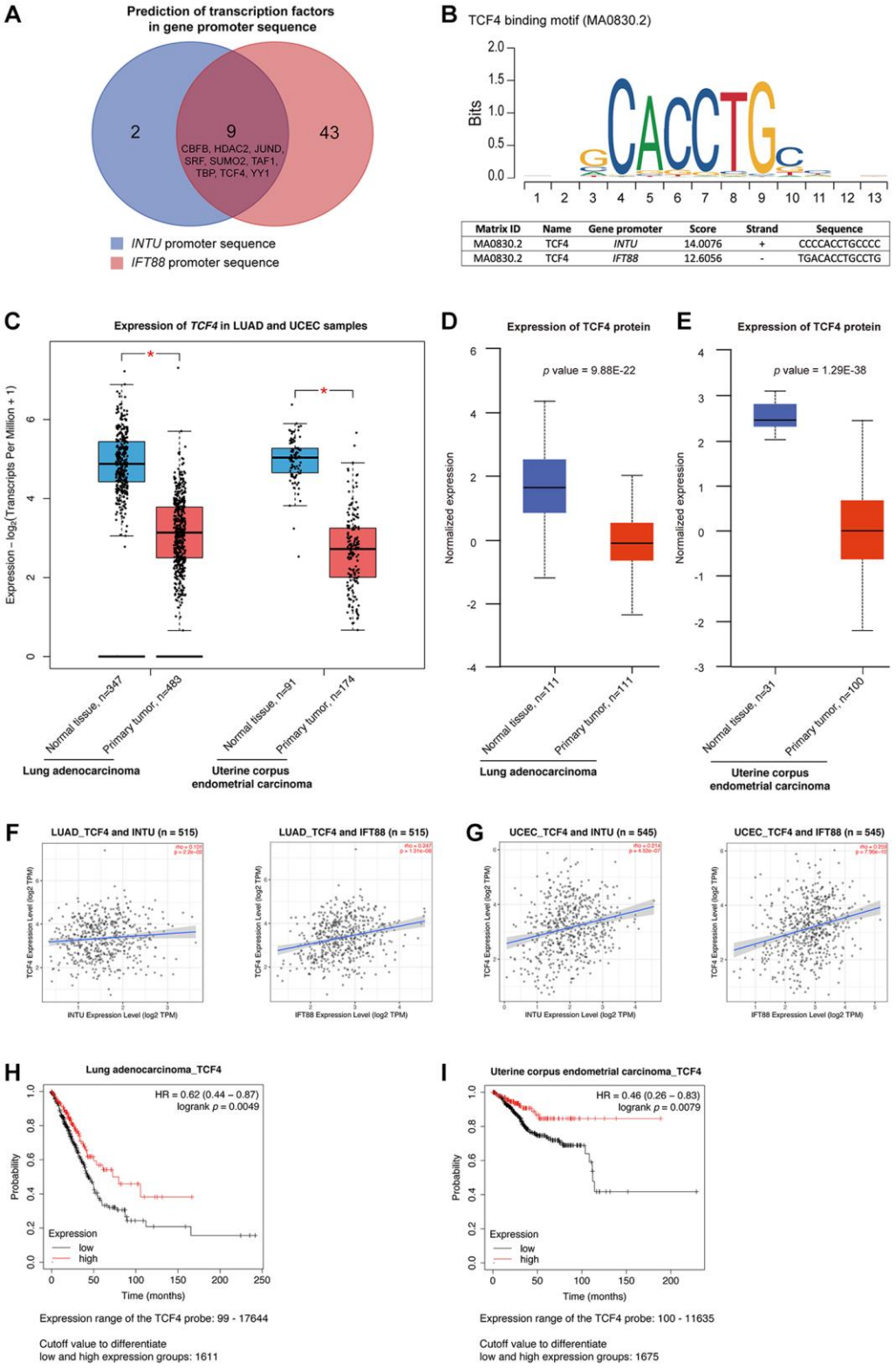

Figure 4. TCF4 was identified as a potential transcription factor that mediates *INTU* and *IFT88* downregulation in LUAD and UCEC tumor samples. (**A**) Nine common transcription factors, including CBFB, HDAC2, JUND, SRF, SUMO2, TAF1, TBP, TCF4 and YY1 were predicted in *INTU* and *IFT88* gene promoters. (**B**) Illustration of TCF4 binding consensus sequence and the putative TCF4 binding sites in *INTU* and *IFT88* promoter sequence. (**C**) The *TCF4* transcript level was downregulated in LUAD and UCEC tumor samples. * denotes $p < 0.05$. (**D**, **E**) The protein level of TCF4 was downregulated in LUAD (**D**) and UCEC (**E**) tumor samples. (**F**, **G**) The expression of *TCF4* positively correlated with the expression of *INTU* and *IFT88* in LUAD (**F**) and UCEC (**G**) tumor samples. (**H**, **I**) The LUAD (**H**) and UCEC (**I**) patients with lowered level of *TCF4* showed reduced OS probabilities.

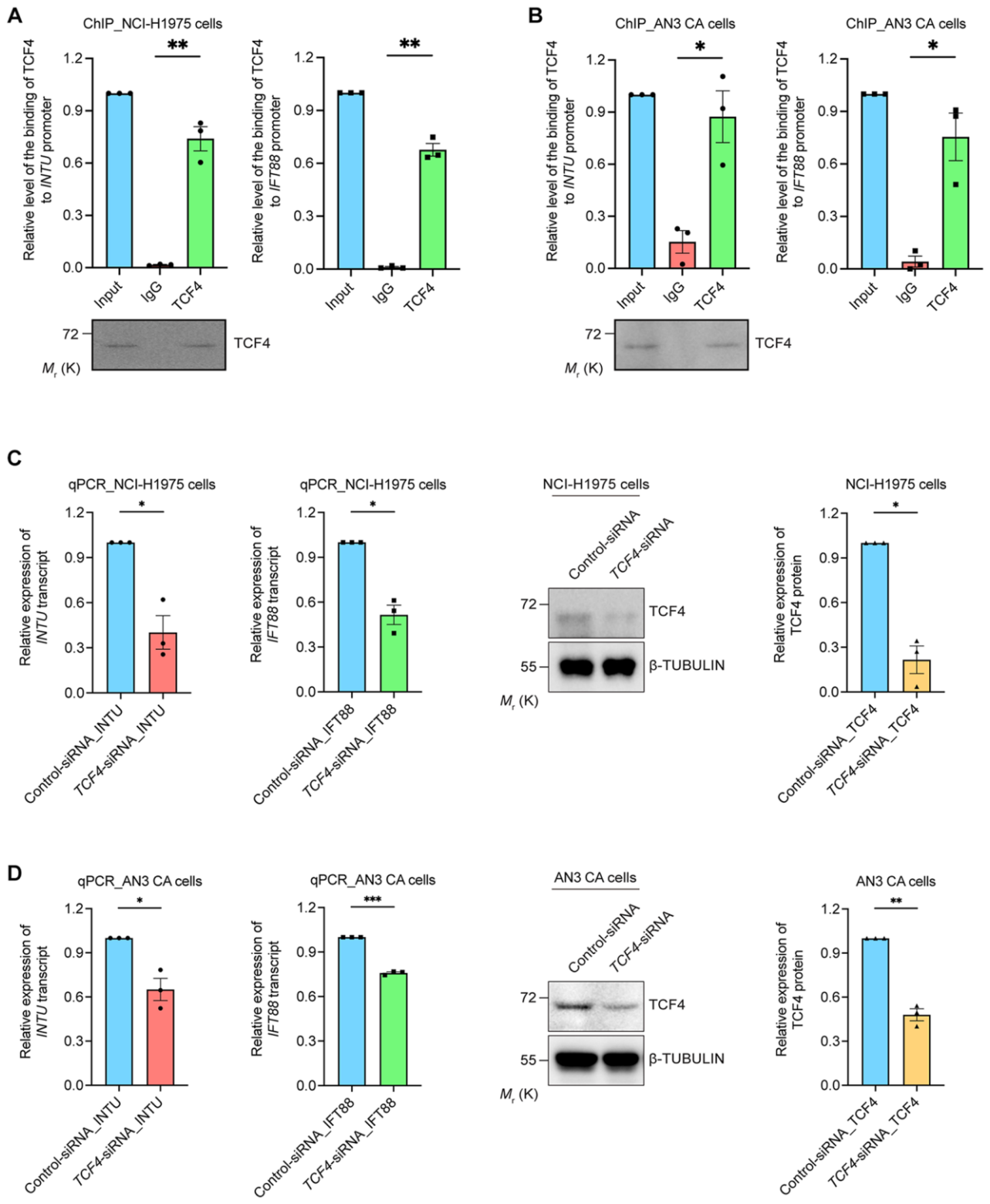

Figure 5. TCF4 interacted with *INTU* and *IFT88* promoters and mediated their gene expression. (**A**, **B**) The binding between TCF4 and *INTU* and *IFT88* promoters was detected in NCI-H1975 (**A**) and AN3 CA (**B**) cells. $n = 3$ biological replicates. Each n represents an independent preparation of ChIP samples. Error bars represent S.E.M. Statistical analysis was performed using two-tailed unpaired Student's *t*-test. * denotes $p < 0.05$ and ** denotes $p < 0.01$. (**C**, **D**) Knockdown of *TCF4* downregulated the transcript levels of *INTU* and *IFT88* in NCI-H1975 (**C**) and AN3 CA (**D**) cells. $n = 3$ biological replicates. Each n represents an independent preparation of RNA and protein samples. Error bars represent S.E.M. Statistical analysis was performed using two-tailed unpaired Student's *t*-test. *denotes $p < 0.05$, **denotes $p < 0.01$ and ***denotes $p < 0.001$.

further support the positive correlation between *TCF4* and *INTU* and *IFT88* levels in LUAD and UCEC samples (Figure 4F, 4G).

Identification of *hsa-miR-212-3p* as the upstream microRNA targeting Hh-related genes *INTU* and *IFT88*

In addition to gene silencing, post-transcriptional regulation of gene expression mediated by non-coding RNAs (ncRNAs), including microRNAs (miRNAs) and long non-coding RNAs (lncRNAs), has been reported [17, 18]. The DIANA-TarBase v8 database was used to select potential miRNAs that target *INTU* or *IFT88* based on experimental evidence [19]. We identified 23 miRNAs that target the *INTU* transcript and four miRNAs that target the *IFT88* transcript (Figure 6A). Interestingly, two miRNAs, *hsa-miR-210-3p* [20] and *hsa-miR-212-3p* [21], were shown to target both *INTU* and *IFT88* (Figure 6A, 6B). We next evaluated the

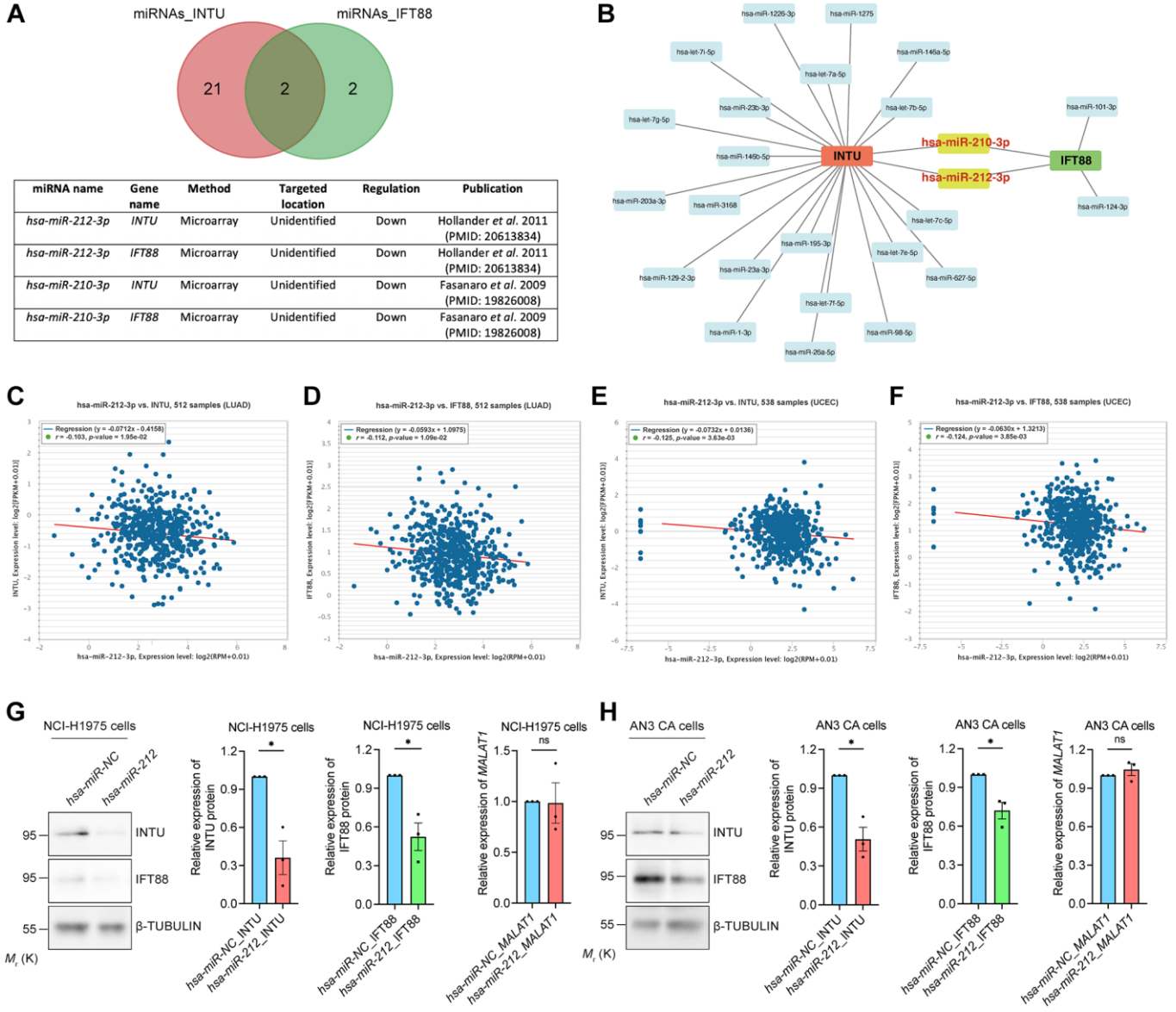

miRNA name	Gene name	Method	Targeted location	Regulation	Publication
hsa-miR-212-3p	*INTU*	Microarray	Unidentified	Down	Hollander *et al.* 2011 (PMID: 20613834)
hsa-miR-212-3p	*IFT88*	Microarray	Unidentified	Down	Hollander *et al.* 2011 (PMID: 20613834)
hsa-miR-210-3p	*INTU*	Microarray	Unidentified	Down	Fasanaro *et al.* 2009 (PMID: 19826008)
hsa-miR-210-3p	*IFT88*	Microarray	Unidentified	Down	Fasanaro *et al.* 2009 (PMID: 19826008)

Figure 6. Identification of *hsa-miR-212-3p* as a communal miRNA against *INTU* and *IFT88* in LUAD and UCEC samples. (**A**) Identification of *hsa-miR-212-3p* and *hsa-miR-210-3p* miRNAs that target both *INTU* and *IFT88* transcripts. (**B**) Construction of the miRNA-target gene regulatory network. (**C**, **D**) The expression of *hsa-miR-212-3p* negatively correlated with the expression of *INTU* (**C**) and *IFT88* (**D**) in LUAD samples. (**E**, **F**) The expression of *hsa-miR-212-3p* negatively correlated with the expression of *INTU* (**E**) and *IFT88* (**F**) in UCEC samples. (**G**, **H**) Overexpression of *hsa-miR-212* led to the downregulation of INTU and IFT88 protein levels in NCI-H1975 (**G**) and AN3 CA (**H**) cells. The *MALAT1* levels were not affected. *n* = 3 biological replicates. Each *n* represents an independent preparation of protein or RNA samples. Error bars represent S.E.M. Statistical analysis was performed using two-tailed unpaired Student's *t*-test. ns indicates no significant difference. * denotes $p < 0.05$.

correlation between the miRNA level and *INTU* or *IFT88* expression in LUAD and UCEC tumor samples. The expression of *hsa-miR-212-3p*, but not *hsa-miR-210-3p*, was found to be negatively correlated with the expression of *INTU* and *IFT88* in LUAD and UCEC samples (Figure 6C–6F and Supplementary Figure 3). Moreover, we found that when *hsa-miR-212* was overexpressed in NCI-H1975 and AN3 CA cells, downregulation of INTU and IFT88 protein levels were detected (Figure 6G, 6H). This further suggests the negative regulatory function of *hsa-miR-212* on the expression of INTU and IFT88.

Identification of *MALAT1* as an upstream lncRNA

We next examined upstream lncRNAs using the DIANA-LncBase v3 database. A total of 63 lncRNAs were obtained, and their expression levels in LUAD and UCEC samples were evaluated (Figure 7A). The levels of four of the 63 lncRNAs, including *HOXA transcript antisense RNA, myeloid-specific 1* (*HOTAIRM1*), *KMT2E antisense RNA 1* (*KMT2E-AS1*), *metastasis associated lung adenocarcinoma transcript 1* (*MALAT1*) and *nuclear paraspeckle assembly transcript 1* (*NEAT1*), were significantly downregulated in LUAD and UCEC tumor samples when compared with their respective normal tissues (Figure 7B and Supplementary Figure 4A). The prognostic significance of these four lncRNAs were further evaluated. We found that *MALAT1*, but not *HOTAIRM1* and *NEAT1*, showed prognostic significance in both LUAD and UCEC patients (Figure 7C, 7D and Supplementary Figure 4B). Similar to what was detected regarding *INTU* (Figure 1) and *IFT88* (Figure 3C, 3D), the reduced level of *MALAT1* contributed to poor OS probabilities in LUAD and UCEC patients (Figure 7C, 7D). Overexpression of *hsa-miR-212* did not modulate *MALAT1* levels in NCI-H1975 and AN3 CA cells (Figure 6G, 6H). In contrast, *MALAT1* has been shown to target *hsa-miR-212-3p* in two independent studies (Figure 7E) [22, 23]. Moreover, the expression of *MALAT1* was found to be positively associated with the mRNA levels of *INTU* and *IFT88* in LUAD and UCEC tumor samples (Figure 7F, 7G). To further validate the regulatory function of *MALAT1* on the expression of INTU and IFT88, *MALAT1* was overexpressed in NCI-H1975 or AN3 CA cells (Figure 7H, 7I). We found that in *MALAT1*-overexpressing cells, the protein levels of INTU and IFT88 were simultaneously increased (Figure 7H, 7I). These results therefore confirm the role of *MALAT1* in regulating the expression of INTU and IFT88 in lung and endometrial cancer cells.

DISCUSSION

In this study, we demonstrated that the downregulation of the *INTU* and *IFT88* was correlated with reduced survival probabilities in LUAD and UCEC patients (Figures 1, 3C, 3D). We next sought to explore the driving forces causing this downregulation in LUAD and UCEC tumor samples, and identified multifaceted mechanisms in the DNA, RNA and protein levels contributing to *INTU* and *IFT88* downregulation (Figures 3–7). This study provides a comprehensive mechanistic investigation regarding *INTU* and *IFT88* downregulation in cancer, and further highlights the involvement of Hh signaling in carcinogenesis.

The dysregulation of Hh signaling has been documented in multiple types of cancer. In BCC, medulloblastoma and rhabdomyosarcoma, mutations in Hh-related genes activate Hh signaling in support of the over-proliferation and tissue invasion of cancer cells [24–26]. In addition to genetic mutation, epigenetic modification also contributes to aberrant Hh signaling in tumor samples. For example, the hypermethylation of *hedgehog-interacting protein* (HHIP), a gene encodes for a negative regulator of Hh signaling, was determined in pancreatic cancer samples. This leads to the reduced expression of HHIP, followed by the upregulation of Hh signaling [27]. In the majority of solid tumors, including colorectal cancer (CRC), the mutation in Hh-related genes was rarely detected [28]. Interestingly, in CRC, the stromal Hh pathway targets were found downregulated despite the increased expression of Hh ligand. This might be due to the insensitivity of stromal cells to epithelial Hh ligand, or the impairment of tissue architecture in tumor stroma [29, 30]. In addition, the restoration of stromal Hh signaling markedly alleviated tumorigenesis, whereas inhibition of Hh signaling exacerbated tumor progression [31]. These findings taken together suggest multiple mechanisms in contributing to the dysregulation of Hh signaling in different cancers, and also highlight the oncogenic role of Hh signaling. Here, we reported two subsets of enriched Hh pathway-associated genes with similar downregulation expression patterns in LUAD and UCEC tumor samples (Figure 2D, 2E). We further showed that lowered levels of *INTU*, *IFT88* or *MKS1* were correlated with decreased OS probabilities in LUAD patients, while UCEC patients with reduced *INTU*, *IFT88* or *IFT140* levels had a poor prognosis (Figures 1, 3C, 3D, Supplementary Figure 5A, 5B). INTU was found to be necessary for the ciliary recruitment of IFT-A proteins, and MKS1 functionally associates with IFT complexes in mediating the transport of cargo proteins to support ciliary outgrowth [8, 32]. Depletion of *INTU* or IFT machinery components leads to ciliogenesis defects [12, 33, 34]. Importantly, the loss of ciliary structures has been recorded in lung and endometrial cancer patient samples [35, 36]. Moreover, stimulation of ciliogenesis has been reported to combat against lung cancer cell

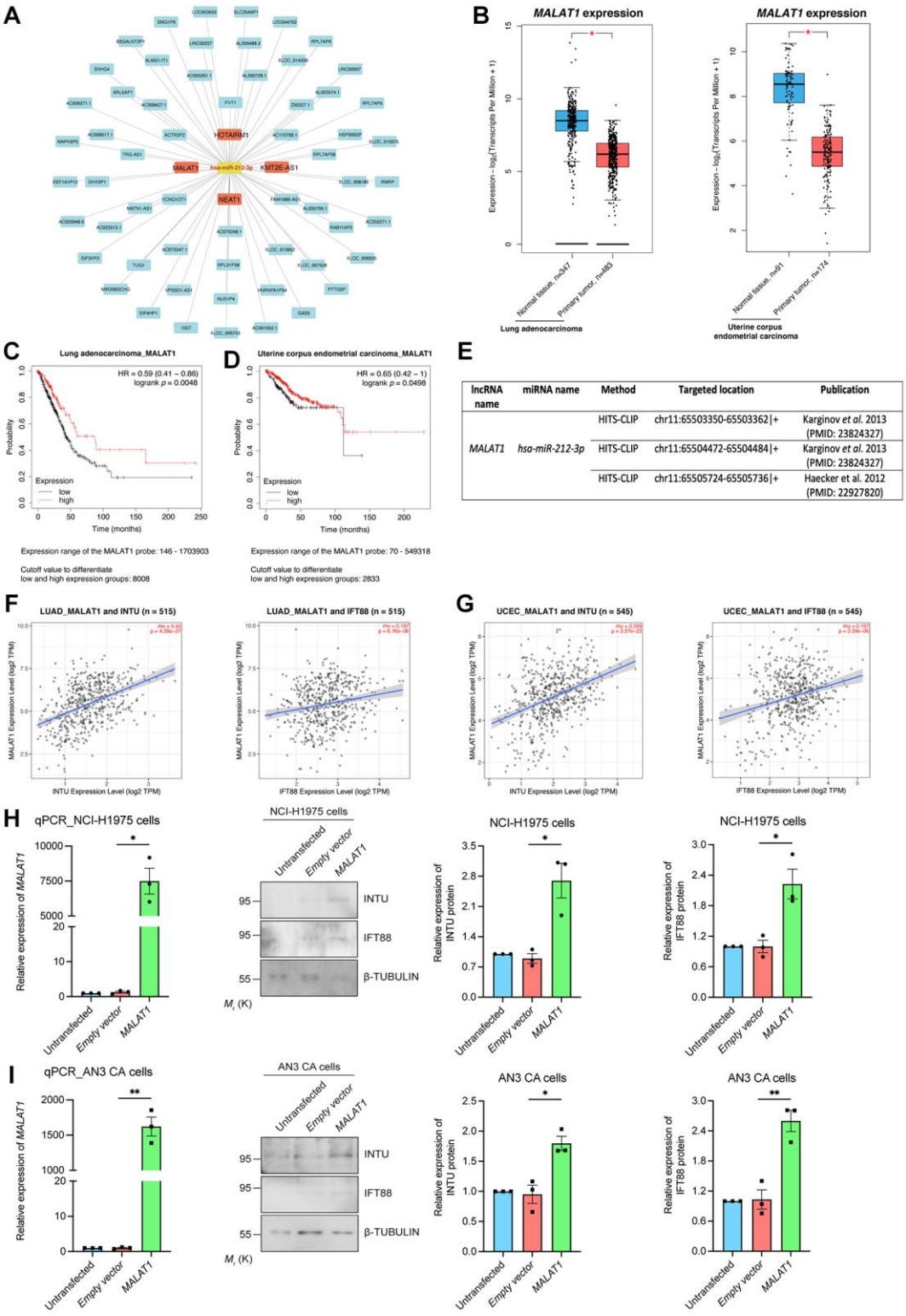

Figure 7. Identification of *MALAT1* as a communal lncRNA mediating *INTU* and *IFT88* expression in LUAD and UCEC samples. (**A**) Identification of the lncRNAs against *hsa-miR-212-3p* and construction of the lncRNA-miRNA regulatory network. (**B**) The expression of *MALAT1* was significantly downregulated in LUAD and UCEC tumor samples. (**C**, **D**) Decreased level of *MALAT1* was found associated with poor prognosis in LUAD (**C**) and UCEC (**D**) patients. (**E**) The *MALAT1* was identified as targeted lncRNA against *hsa-miR-212-3p* from two independent studies. (**F**, **G**) The expression of *MALAT1* positively associated with the expression of *INTU* and *IFT88* in LUAD (**F**) and UCEC (**G**) tumor samples. (**H**, **I**) Overexpression of *MALAT1* caused the upregulation of INTU and IFT88 protein levels in NCI-H1975 (**H**) and AN3 CA (**I**) cells. *n* = 3 biological replicates. Each *n* represents an independent preparation of RNA and protein samples. Error bars represent S.E.M. Statistical analysis was performed using two-tailed unpaired Student's *t*-test. * denotes $p < 0.05$.

proliferation, invasion and epithelial-mesenchymal transition [37]. These findings therefore indicate that disruption of Hh signaling components might cause ciliogenesis defects, which in favour of oncogenesis in LUAD and UCEC tissues.

TCF4 belongs to the helix–loop–helix (HLH) family of proteins ubiquitously expressed throughout different human tissues [38]. A basic residue group on the TCF4 N-terminus is critical for its DNA-binding function, while the C-terminal HLH domain mediates the dimerization of TCF4 when it binds to DNA [39]. Several studies have demonstrated the association between TCF4 function and DNA methylation [40, 41]. Specifically, TCF4 was correlated with DNA hypo-methylation in mammalian epithelial stem cells. Upon conditional knockout of *TCF4*, the TCF4-bound differentially methylated DNA sequence was found to be strongly methylated [41]. Interestingly, when looking into the TCF4 binding site in the *INTU* promoter sequence, we found that the TCF4 site resides in the $INTU^{CpG}$ (highlighted in Supplementary Table 2). The methylation level of $INTU^{CpG}$ was upregulated in LUAD and UCEC samples (Figure 3G). Reduction of the TCF4 protein level was recorded in both LUAD and UCEC tumor samples (Figure 4D). Such attenuation of the TCF4 level might result in $INTU^{CpG}$ hypermethylation, which in turn leads to the downregulation of *INTU* expression in LUAD and UCEC samples. Meanwhile, TCF4 did not associate with $IFT88^{CpG}$ (Supplementary Table 2), and no significant change in $IFT88^{CpG}$ methylation level was detected in LUAD and UCEC samples (Figure 3H).

Genetic mutations in *TCF4* have been reported in neurological disorders, including Fuchs's corneal dystrophy [42], Pitt–Hopkins syndrome [43], and schizophrenia [44], as well as non-neurological diseases, including primary sclerosing cholangitis [45] and sporadic Sonic Hedgehog-associated medulloblastoma (SHH MB) [46]. Functional analysis was carried out on mutant TCF4 proteins harboring the mutations identified from SHH MB patients. Experimental findings highlighted the loss-of-function behind these TCF4 mutations, as exemplified by the fact that mutant TCF4 proteins failed to inhibit the proliferation of medulloblastoma cells, unlike the wild-type TCF4 protein [40, 47]. We also found a nonsense mutation at the arginine 174 residue ($R174^{*}$) on the TCF4 protein in eight UCEC patient samples (Supplementary Figure 6A, 6B), and the R174 site was conserved across different species (Supplementary Figure 6C). This nonsense mutation generates a truncated TCF4 protein which lacks the C-terminal HLH motif that is crucial for mediating gene transcription, suggesting the loss of TCF4 trans-activating function due to the presence of such a mutation. This could serve as another mechanism leading to the downregulation of Hh-related genes in UCEC tumor samples. Interestingly, a similar $TCF4^{R174*}$ mutation was previously reported in patients with SHH MB and Pitt–Hopkins syndrome [46, 47], suggesting that the communal loss-of-function mechanism is involved in a broad spectrum of human disorders.

miRNAs and lncRNAs are two major subtypes of ncRNAs associated with the well-documented ceRNA mechanism that is essential for controlling gene expression at a post-transcriptional level [18, 48]. We identified a novel and communal *MALAT1-hsa-miR-212-3p* regulatory network that downregulated *INTU* and *IFT88* expression in LUAD and UCEC samples (Figure 5). The recurrent fusion of *MALAT1* with the *GLI1* gene was reported in patients with gastroblastoma and plexiform fibromyxoma [49, 50]. This *MALAT1-GLI1* fusion mutation activated Hh signaling and consequently led to malignant tumor formation, suggesting a relationship between *MALAT1* function and Hh signaling activity [49, 51, 52]. In this study, we further highlighted the involvement of *MALAT1* in regulating Hh pathway-associated genes. We found that in addition to *INTU* and *IFT88*, other Hh-related genes with similar expression profiles as *INTU* were also enriched in LUAD and UCEC samples (Figure 2D, 2E). Interestingly, the expression of *hsa-miR-212-3p* was negatively associated with the expression of *MKS1* and *WDR90* in LUAD samples (Supplementary Figure 7A) and *DYNC2H1*, *IFT140* and *WDR19* in UCEC samples (Supplementary Figure 7B). Positive correlations were determined between *MALAT1*, *MKS1* and *WDR90* in LUAD samples and *MALAT1*, *DYNC2H1* and *WDR19* in UCEC samples (Supplementary Figure 7C, 7D). Taken together, these findings emphasize the *MALAT1-hsa-miR-212-3p* network as a master upstream regulator targeting downstream Hh pathway-associated genes in LUAD and UCEC tumor samples. In addition, *MALAT1* binds to active chromatin sites and regulates gene transcription by recruiting chromatin modifiers or transcription regulators to specific genomic loci [53, 54]. This might be an alternative mechanism that accounts for *MALAT1*'s regulation on Hh pathway-associated gene expression and is worthy to be further investigated.

Several recent studies have reported the anti-tumorigenesis role of TCF4 in colorectal carcinoma and SHH MB [47, 55]. TCF4 is capable of attenuating the proliferation of colon cancer and medulloblastoma cells, whereas loss of *TCF4* exerts the opposite effect, favoring tumorigenesis [47, 56, 57]. The effect of *MALAT1* on tumor cell growth and invasion is controversial. Although the oncogenic functions of *MALAT1* have been reported in malignancies such as colorectal and liver cancer [58, 59], more recent studies

Table 1. Summary of *MALAT1* small molecule activators.

lncRNA	Small molecules	Effect on lncRNA expression	Approved by FDA	Validated by experiments	Validation method	Experimental material	References
MALAT1	Carboplatin + Docetaxel	Up-regulation	Yes	Yes	Quantitative real-time PCR	Ovarian cancer cell line	[81]
MALAT1	Quercetin	Up-regulation	Yes	Yes	Quantitative real-time PCR	Rheumatoid arthritis fibroblast-like synoviocytes	[82]

have highlighted the tumor suppressive role of *MALAT1* against the growth and metastasis of glioma and breast cancer cells [60, 61]. These findings taken together suggest a cancer type-dependent role of *MALAT1* in tumorigenesis. Given the functions of TCF4 and *MALAT1* as tumor suppressors, targeting the functional elevation of TCF4 and *MALAT1* could be therapeutically beneficial against tumorigenesis. In fact, the identification of small molecule drugs aimed at stimulating TCF4 function is now under investigation (Pitt Hopkins Research Foundation; https://pitthopkins.org/portfolio-item/pilot-study-to-identify-small-molecule-activators-of-tcf4-as-a-treatment-for-pitt-hopkins-syndrome/). Meanwhile, different small molecule activators for *MALAT1* have been reported (Table 1). A combinatorial drug treatment has been demonstrated as an effective therapeutic strategy in combating carcinogenesis [62–64]. The use of both TCF4 and *MALAT1* activators in the treatment against LUAD and UCEC would be an interesting topic worthy of further exploration.

In summary, we showed that the downregulation of the Hh pathway-associated genes *INTU* and *IFT88* was correlated with poor prognosis in LUAD and UCEC patients. Moreover, we demonstrated novel TCF4 and ncRNA-involved mechanisms that contribute to the downregulation of *INTU* and *IFT88* in LUAD and UCEC tumor samples (Figure 8). We further propose that a treatment strategy that simultaneously targets TCF4 and

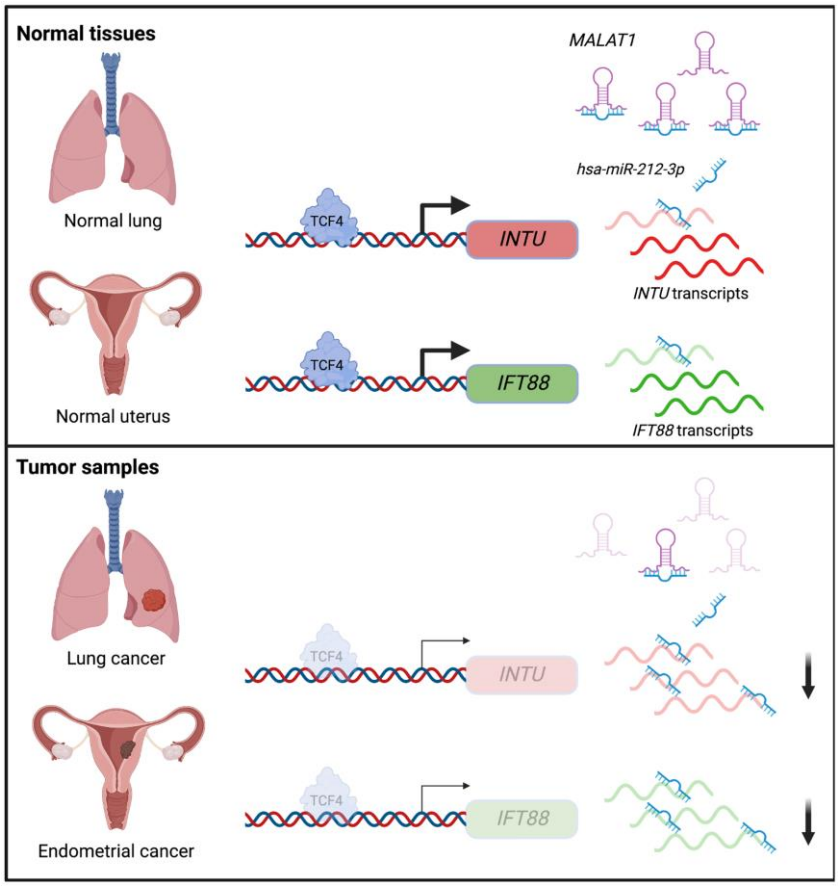

Figure 8. Illustration of the underlying mechanisms that contribute to *INTU* and *IFT88* downregulation in the lung and endometrial cancers.

MALAT1 to enrich *INTU* and *IFT88* might be a promising therapeutic intervention against LUAD and UCEC.

MATERIALS AND METHODS

Kaplan-Meier plotter analysis

The pan-cancer analysis function (https://kmplot.com/analysis/index.php?p=service&cancer=pancancer_rnaseq) from the Kaplan-Meier plotter database was used to evaluate the prognostic significance of *INTU* mRNA expression in 21 different types of cancer [65]. The prognostic significance of Hh pathway-associated genes *IFT88*, *MKS1*, *WDR90*, *IFT140*, *DYNC2H1* and *WDR19* was also evaluated using LUAD and UCEC patient survival data from Kaplan-Meier plotter database. Similar approach was used to determine the prognostic value of TCF4 and lncRNAs. The OS probabilities of cancer patients were assessed using the Kaplan-Meier survival plots, and logrank $p < 0.05$ indicates that the association between gene/lncRNA expression and patient survival probability is statistically significant.

GEPIA2 database analysis

GEPIA2 (http://gepia2.cancer-pku.cn/#index) is an online database that provides gene expression profiling and interactive analyses in primary tumor and normal tissue samples on the basis of data from The Cancer Genome Atlas (TCGA) and the Genotype-Tissue Expression (GTEx) projects [66]. The expression of *INTU*, housekeeping genes, different transcription factors and different lncRNAs were determined in LUAD and UCEC primary tumor samples and their respective normal tissues. The $p < 0.05$ was considered as statistically significant. The top 100 genes with similar expression pattern as *INTU* in LUAD or UCEC tumor samples were also selected using the "Similar Gene Detection" function from GEPIA2. The detailed gene lists are included in Supplementary Table 1.

Gene ontology and Reactome pathway analysis

The *INTU* and top 100 genes with similar expression pattern obtained from GEPIA2 database were input to Database for Annotation, Visualization and Integrated Discovery (DAVID) v6.8 (https://david.ncifcrf.gov/home.jsp) to analyze their enriched Gene Ontology (GO) terms and Reactome pathways [67]. The biological processes (BP) and cellular components (CC) were included in the GO enrichment analysis. The false discovery rate (FDR) *q*-value < 0.05 was used as selection criteria for significantly enriched GO terms and Reactome pathways.

Protein-protein interaction (PPI) network analysis

The construction of PPI network was performed using STRING v11.5 database (https://string-db.org/) [68]. The genes with similar expression pattern obtained from GEPIA2 database were input to STRING database, and the PPI network was constructed based on the sources of "Co-expression", "Databases", "Experiments", "Gene Fusion", "Neighborhood" and "Textmining" with minimum required interaction score of medium confidence. The Cytoscape v3.8.0 was used to visualize the constructed PPI network [69].

Prediction of CpG islands and transcription factor binding sites within gene promoter sequences

INTU and *IFT88* promoter sequences were withdrawn from GenBank under the accession numbers NC_000004.12 and NC_000013.11, respectively. The CpG islands were predicted using MethPrimer 2.0 (http://www.urogene.org/cgi-bin/methprimer2/MethPrimer.cgi) software [70]. The transcription factor binding sites were predicted using Animal Transcription Factor Database 3.0 (AnimalTFDB3.0; http://bioinfo.life.hust.edu.cn/AnimalTFDB/#!/) [71]. The "*q*-value < 0.05" and "Score > 20" were used as filtering parameters to select potential transcription factors for *INTU* and *IFT88*. The TCF4 binding site was further validated using JASPAR (https://jaspar.genereg.net/) database [72]. The relative profile score threshold equals to 90%, and "Score > 12.5" and "Relative score > 0.92" were used as filtering parameters. The detailed *INTU* and *IFT88* promoter sequences are listed in Supplementary Table 2, the putative CpG islands are shown in blue and the TCF4 binding sites are highlighted.

MethHC2.0 database analysis

MethHC2.0 is a web-based resource that provides analysis on the methylation levels of gene regions, including CpG islands, from different types of cancer [73]. The methylation levels of *INTU* and *IFT88* CpG islands were scrutinized using methylome data from LUAD and UCEC tumor samples and their respective normal samples.

UALCAN database analysis

UALCAN (http://ualcan.path.uab.edu/analysis-prot.html) is an interactive online resource that enables the analysis of protein expression based on the Clinical Proteomic Tumor Analysis Consortium Confirmatory/Discovery datasets [74]. In this study, the TCF4 protein expression from LUAD and UCEC tumor

samples and their respective normal tissues was analyzed.

Candidate miRNA and lncRNA prediction

The list of miRNAs that target *INTU* and *IFT88* was obtained using DIANA-Tarbase v8 database (https://dianalab.e-ce.uth.gr/html/diana/web/index.php?r=tarbasev8%2Findex) [19]. The "Species = *Homo Sapiens*" and "Validated as Positive" were used as filtering parameters. The miRNA-target genes regulatory network was constructed using Cytoscape v3.8.0.

The list of lncRNAs that target different miRNAs was obtained using DIANA-LncBase v3 database (https://diana.e-ce.uth.gr/lncbasev3) [75]. The "Species = *Homo Sapiens*", "miRNA Conf. Level = High" and "Validated as Positive" were used as filtering parameters. The lncRNA-miRNA regulatory network was constructed using Cytoscape v3.8.0.

ENCORI database analysis

ENCORI (http://starbase.sysu.edu.cn/) is an online database that determines the correlation between miRNA level and target gene expression [76]. The expression correlation between *hsa-miR-210-3p*/*hsa-miR-212-3p* and different enriched Hh-related genes was analyzed using "miRNA-Target CoExpression" module from the "Pan-Cancer" function. The *p*-value < 0.05 was considered as statistically significant.

TIMER2.0 database analysis

The TIMER2.0 (http://timer.cistrome.org/) is an online web server that enables the detection of gene expression correlation [77]. The correlation among different Hh-related genes, and correlation between Hh-related genes and *MALAT1* in LUAD and UCEC tumor samples were evaluated using the "Gene_Correlation" module. No adjustment was made, and $p < 0.05$ was considered as statistically significant.

cBioPortal database analysis

cBioPortal v3.7.3 is a comprehensive web resource that enables the visualization and analysis of cancer genomic mutation data (https://www.cbioportal.org/) [78, 79]. The missense and nonsense mutation profiles in *INTU*, *IFT88* and *TCF4* genes were obtained from Lung Adenocarcinoma (TCGA, PanCancer Atlas, 566 samples) and Uterine Corpus Endometrial Carcinoma (TCGA, PanCancer Atlas, 529 samples) datasets.

D-lnc database

The D-lnc database (http://www.jianglab.cn/D-lnc/index.jsp) is a comprehensive platform that summarizes the lncRNA-targeting drugs based on the experimental evidence and computational predictions [80]. The "Species = *Homo Sapiens*" and "lncRNA = *MALAT1*" were used to select potential small molecules that target *MALAT1*.

Mammalian cell culture

The human endometrial adenocarcinoma cell line AN3 CA was a kind gift from Prof. Chi Chiu Wang (Department of Obstetrics and Gynecology, The Chinese University of Hong Kong, China). The human lung adenocarcinoma cell line NCI-H1975 (CRL-5908™) was obtained from American Type Culture Collection. Both cell lines were cultured using Dulbecco's Modified Eagle's Medium (11995065, Thermo Fisher Scientific) supplemented with 10% fetal bovine serum (F7524, Sigma-Aldrich) and 1% penicillin-streptomycin solution (15140122, Thermo Fisher Scientific). The cells were maintained in a 37°C humidified cell culture incubator supplemented with 5% CO_2.

Plasmid, microRNA and siRNA transfection

The *pcDNA-MALAT1* plasmid was a kind gift from Prof. Huating Wang (Department of Orthopaedics and Traumatology, The Chinese University of Hong Kong, China). Cells were transfected with 0.5 μg *pcDNA-MALAT1* plasmid with 0.5 μl lipofectamine 2000 (11668019, Thermo Fisher Scientific). The RNA or protein samples were harvested 24 h post transfection. The *hsa-miR-NC* (4464058) and *hsa-miR-212* (4464066) were synthesized by Thermo Fisher Scientific. Cells were transfected with 20 pmol microRNAs with 2 μl lipoRNAiMAX (13778150, Thermo Fisher Scientific). Cell culture medium and transfection mixtures were refreshed every 24 h, and protein samples were harvested 72 h post transfection. The Control-siRNA, 5′-UUCUCCGAACGUGUCACGUTT-3′ and *TCF4*-siRNA, 5′-CUAUCAGUAUUCUAGCAAUAATT-3′ were synthesized by Sangon Biotech (Shanghai) Co., Ltd. Cells were transfected with 20 pmol siRNAs with 2 μl lipoRNAiMAX. Cell culture medium and transfection mixtures were refreshed every 24 h, and RNA or protein samples were harvested 72 h post transfection.

Drug treatment

The NCI-H1975 and AN3 CA cells were treated with 2 μM 5-azacytidine (A2385, Sigma-Aldrich). The

treatment lasted 72 h, with medium and drug refreshed every 24 h.

Chromatin immunoprecipitation

The chromatin immunoprecipitation (ChIP) assay was performed using Pierce™ Magnetic ChIP Kit (26157, Thermo Fisher Scientific). The experimental procedures were carried out following the manufacturer's instructions. Two micrograms of anti-TCF4 antibody (ab217668, abcam) were used for the immunoprecipitation, while the same amount of normal rabbit IgG (I-1000, Vector Laboratories, lnc.) was used as negative control. Twenty nanograms of recovered genomic DNAs from each of input, normal rabbit IgG and TCF4 immunoprecipitated samples were used in the following real-time PCR to analyze the levels of *INTU* and *IFT88* promoter fragments. The primers used were *INTU promoter-F*, 5′-CAGCCTGGACTTCGCGAG-3′; *INTU promoter-R*, 5′-TGAAGGCGGTGGTGTCAG-3′; *IFT88 promoter-F*, 5′-AAAACGGACACCTTAA GCGC-3′ and *IFT88 promoter-R*, 5′-CTTGTGAA CCTTGGAAGCCC-3′.

RNA extraction, reverse transcription and real-time PCR

The total RNA was isolated from cultured cells using TRIzol™ reagent (15596018, Thermo Fisher Scientific). The reverse transcription was performed using ImProm-II™ Reverse Transcription System (A3803, Promega) and random hexamer (N8080127, Thermo Fisher Scientific) according to the manufacturers' instructions. Quantitative real-time PCR was performed using SYBR™ Green PCR Master Mix (4309155, Thermo Fisher Scientific) on the Bio-Rad CFX96 system. Relative gene expression was determined via normalizing against *β-ACTIN* using the $2^{-\Delta\Delta CT}$ method. Primers used in this study were *INTU-F*, 5′-CGCATAGATGAACGGCTAGC-3′; *INTU-R*, 5′-AGCGTTCTTCTGCATGTTGG-3′; *IFT88-F*, 5′-CTGCAACCAATCTCTCAGCC-3′; *IFT88-R*, 5′-GCGGCCTTCTCATAATCACC-3′; *MALAT1-F*, 5′-ATGCGAGTTGTTCTCCGTCT-3′; *MALAT1-R*, 5′-TATCTGCGGTTTCCTCAAGC-3′; *β-ACTIN-F*, 5′-ATGTGCAAGGCCGGTTTCGC-3′ and *β-ACTIN-R*, 5′-CGACACGCAGCTCATTGTAG-3′.

Immunoblotting

Protein samples were harvested from cells using the SDS sample buffer (100 mM Tris-HCl, pH 6.8, 2% SDS, 40% glycerol, 5% β-mercaptoethanol, and 0.1% bromophenol blue). Samples were heated at 99°C for 10 min prior to being subjected to the immunoblot analysis. The protein samples were then transferred to a PVDF membrane (IPVH00010, pore size 0.45 μm, Merck Millipore). The membrane was blocked using 5% nonfat milk at 25°C for 1 h, followed by the incubation of primary antibodies at 4°C for 16 h. Primary antibodies used were anti-TCF4 (ab217668, 1:1,000, abcam), anti-INTU (ab229243, 1:1,000, abcam), anti-IFT88 (13967-1-AP, 1:1,000, Proteintech) and anti-β-TUBULIN (ab6046, 1:2,000, abcam). The membrane was washed three times with 1× TBST each for 10 min, before being subjected to the incubation of secondary antibodies at 25°C for 1 h. Secondary antibodies used were HRP-conjugated goat anti-rabbit IgG (H + L) (11-035-045, 1:5,000) and HRP-conjugated goat anti-mouse IgG (H + L) (115-035-062, 1:10,000) from Jackson ImmunoResearch. The membrane was washed three times with 1× TBST each for 10 min, prior to the detection of chemiluminescent signal. The signal was developed using Immobilon Forte Western HRP substrate (WBLUF0100, Merck Millipore), and the images were captured and processed using ChemiDoc™ Touch Imaging System (170-8370, Bio-Rad).

Statistical analysis

The two-tailed, unpaired Student's *t* test was used for the comparison between two experimental groups. *, ** and *** represent $p < 0.05$, $p < 0.01$ and $p < 0.001$, respectively, which are considered statistically significant. ns indicates no significant difference. GraphPad Prism version 9.0.0 was used for statistical analysis.

AUTHOR CONTRIBUTIONS

Z.S.C. designed research, performed experiments and analyzed the data, H.Y.E.C. and Z.S.C. wrote and revised the paper.

ACKNOWLEDGMENTS

The human endometrial adenocarcinoma cell line AN3 CA was a kind gift from Prof. Chi Chiu Wang (Department of Obstetrics and Gynecology, The Chinese University of Hong Kong, China). The *pcDNA-MALAT1* plasmid was a kind gift from Prof. Huating Wang (Department of Orthopaedics and Traumatology, The Chinese University of Hong Kong, China).

CONFLICTS OF INTERESTS

The authors declare no conflicts of interest related to this study.

ETHICAL STATEMENT

Biological and chemical safety approval for this study (14122815) was obtained from the Chinese University of Hong Kong.

FUNDING

Zhefan Stephen Chen was supported by a Postdoctoral Fellowship in Clinical Neurosciences program between The Chinese University of Hong Kong and University of Oxford (Nuffield Department of Clinical Neurosciences and Pembroke College).

REFERENCES

1. Wu F, Zhang Y, Sun B, McMahon AP, Wang Y. Hedgehog Signaling: From Basic Biology to Cancer Therapy. Cell Chem Biol. 2017; 24:252–80. https://doi.org/10.1016/j.chembiol.2017.02.010 PMID:28286127

2. Niyaz M, Khan MS, Mudassar S. Hedgehog Signaling: An Achilles' Heel in Cancer. Transl Oncol. 2019; 12:1334–44. https://doi.org/10.1016/j.tranon.2019.07.004 PMID:31352196

3. Goetz SC, Anderson KV. The primary cilium: a signalling centre during vertebrate development. Nat Rev Genet. 2010; 11:331–44. https://doi.org/10.1038/nrg2774 PMID:20395968

4. Cui C, Chatterjee B, Lozito TP, Zhang Z, Francis RJ, Yagi H, Swanhart LM, Sanker S, Francis D, Yu Q, San Agustin JT, Puligilla C, Chatterjee T, et al. Wdpcp, a PCP protein required for ciliogenesis, regulates directional cell migration and cell polarity by direct modulation of the actin cytoskeleton. PLoS Biol. 2013; 11:e1001720. https://doi.org/10.1371/journal.pbio.1001720 PMID:24302887

5. Park TJ, Haigo SL, Wallingford JB. Ciliogenesis defects in embryos lacking inturned or fuzzy function are associated with failure of planar cell polarity and Hedgehog signaling. Nat Genet. 2006; 38:303–11. https://doi.org/10.1038/ng1753 PMID:16493421

6. Wheway G, Nazlamova L, Hancock JT. Signaling through the Primary Cilium. Front Cell Dev Biol. 2018; 6:8. https://doi.org/10.3389/fcell.2018.00008 PMID:29473038

7. Taschner M, Lorentzen E. The Intraflagellar Transport Machinery. Cold Spring Harb Perspect Biol. 2016; 8:a028092. https://doi.org/10.1101/cshperspect.a028092 PMID:27352625

8. Toriyama M, Lee C, Taylor SP, Duran I, Cohn DH, Bruel AL, Tabler JM, Drew K, Kelly MR, Kim S, Park TJ, Braun DA, Pierquin G, et al, and University of Washington Center for Mendelian Genomics. The ciliopathy-associated CPLANE proteins direct basal body recruitment of intraflagellar transport machinery. Nat Genet. 2016; 48:648–56. https://doi.org/10.1038/ng.3558 PMID:27158779

9. Skoda AM, Simovic D, Karin V, Kardum V, Vranic S, Serman L. The role of the Hedgehog signaling pathway in cancer: A comprehensive review. Bosn J Basic Med Sci. 2018; 18:8–20. https://doi.org/10.17305/bjbms.2018.2756 PMID:29274272

10. Chen ZS, Lin X, Chan TF, Chan HYE. Pan-cancer investigation reveals mechanistic insights of planar cell polarity gene *Fuz* in carcinogenesis. Aging (Albany NY). 2021; 13:7259–83. https://doi.org/10.18632/aging.202582 PMID:33658400

11. Natanzon Y, Earp M, Cunningham JM, Kalli KR, Wang C, Armasu SM, Larson MC, Bowtell DD, Garsed DW, Fridley BL, Winham SJ, Goode EL. Genomic Analysis Using Regularized Regression in High-Grade Serous Ovarian Cancer. Cancer Inform. 2018; 17:1176935118755341. https://doi.org/10.1177/1176935118755341 PMID:29434467

12. Yang N, Leung EL, Liu C, Li L, Eguether T, Jun Yao XJ, Jones EC, Norris DA, Liu A, Clark RA, Roop DR, Pazour GJ, Shroyer KR, Chen J. INTU is essential for oncogenic Hh signaling through regulating primary cilia formation in basal cell carcinoma. Oncogene. 2017; 36:4997–5005. https://doi.org/10.1038/onc.2017.117 PMID:28459465

13. Deaton AM, Bird A. CpG islands and the regulation of transcription. Genes Dev. 2011; 25:1010–22. https://doi.org/10.1101/gad.2037511 PMID:21576262

14. Jones PA. Functions of DNA methylation: islands, start sites, gene bodies and beyond. Nat Rev Genet. 2012; 13:484–92. https://doi.org/10.1038/nrg3230 PMID:22641018

15. Christman JK. 5-Azacytidine and 5-aza-2'-deoxycytidine as inhibitors of DNA methylation: mechanistic studies and their implications for cancer therapy. Oncogene. 2002; 21:5483–95. https://doi.org/10.1038/sj.onc.1205699 PMID:12154409

16. Lambert SA, Jolma A, Campitelli LF, Das PK, Yin Y, Albu M, Chen X, Taipale J, Hughes TR, Weirauch MT. The Human Transcription Factors. Cell. 2018; 172:650–65.

https://doi.org/10.1016/j.cell.2018.01.029
PMID:29425488

17. O'Brien J, Hayder H, Zayed Y, Peng C. Overview of MicroRNA Biogenesis, Mechanisms of Actions, and Circulation. Front Endocrinol (Lausanne). 2018; 9:402.
https://doi.org/10.3389/fendo.2018.00402
PMID:30123182

18. Statello L, Guo CJ, Chen LL, Huarte M. Gene regulation by long non-coding RNAs and its biological functions. Nat Rev Mol Cell Biol. 2021; 22:96–118.
https://doi.org/10.1038/s41580-020-00315-9
PMID:33353982

19. Karagkouni D, Paraskevopoulou MD, Chatzopoulos S, Vlachos IS, Tastsoglou S, Kanellos I, Papadimitriou D, Kavakiotis I, Maniou S, Skoufos G, Vergoulis T, Dalamagas T, Hatzigeorgiou AG. DIANA-TarBase v8: a decade-long collection of experimentally supported miRNA-gene interactions. Nucleic Acids Res. 2018; 46:D239–45.
https://doi.org/10.1093/nar/gkx1141
PMID:29156006

20. Fasanaro P, Greco S, Lorenzi M, Pescatori M, Brioschi M, Kulshreshtha R, Banfi C, Stubbs A, Calin GA, Ivan M, Capogrossi MC, Martelli F. An integrated approach for experimental target identification of hypoxia-induced miR-210. J Biol Chem. 2009; 284:35134–43.
https://doi.org/10.1074/jbc.M109.052779
PMID:19826008

21. Hollander JA, Im HI, Amelio AL, Kocerha J, Bali P, Lu Q, Willoughby D, Wahlestedt C, Conkright MD, Kenny PJ. Striatal microRNA controls cocaine intake through CREB signalling. Nature. 2010; 466:197–202.
https://doi.org/10.1038/nature09202
PMID:20613834

22. Karginov FV, Hannon GJ. Remodeling of Ago2-mRNA interactions upon cellular stress reflects miRNA complementarity and correlates with altered translation rates. Genes Dev. 2013; 27:1624–32.
https://doi.org/10.1101/gad.215939.113
PMID:23824327

23. Haecker I, Gay LA, Yang Y, Hu J, Morse AM, McIntyre LM, Renne R. Ago HITS-CLIP expands understanding of Kaposi's sarcoma-associated herpesvirus miRNA function in primary effusion lymphomas. PLoS Pathog. 2012; 8:e1002884.
https://doi.org/10.1371/journal.ppat.1002884
PMID:22927820

24. Taylor MD, Liu L, Raffel C, Hui CC, Mainprize TG, Zhang X, Agatep R, Chiappa S, Gao L, Lowrance A, Hao A, Goldstein AM, Stavrou T, et al. Mutations in SUFU predispose to medulloblastoma. Nat Genet. 2002; 31:306–10.
https://doi.org/10.1038/ng916
PMID:12068298

25. Xie J, Murone M, Luoh SM, Ryan A, Gu Q, Zhang C, Bonifas JM, Lam CW, Hynes M, Goddard A, Rosenthal A, Epstein EH Jr, de Sauvage FJ. Activating Smoothened mutations in sporadic basal-cell carcinoma. Nature. 1998; 391:90–2.
https://doi.org/10.1038/34201
PMID:9422511

26. Tostar U, Malm CJ, Meis-Kindblom JM, Kindblom LG, Toftgård R, Undén AB. Deregulation of the hedgehog signalling pathway: a possible role for the PTCH and SUFU genes in human rhabdomyoma and rhabdomyosarcoma development. J Pathol. 2006; 208:17–25.
https://doi.org/10.1002/path.1882
PMID:16294371

27. Martin ST, Sato N, Dhara S, Chang R, Hustinx SR, Abe T, Maitra A, Goggins M. Aberrant methylation of the Human Hedgehog interacting protein (HHIP) gene in pancreatic neoplasms. Cancer Biol Ther. 2005; 4:728–33.
https://doi.org/10.4161/cbt.4.7.1802
PMID:15970691

28. Cancer Genome Atlas Network. Comprehensive molecular characterization of human colon and rectal cancer. Nature. 2012; 487:330–7.
https://doi.org/10.1038/nature11252
PMID:22810696

29. Cohen M, Kicheva A, Ribeiro A, Blassberg R, Page KM, Barnes CP, Briscoe J. Ptch1 and Gli regulate Shh signalling dynamics via multiple mechanisms. Nat Commun. 2015; 6:6709.
https://doi.org/10.1038/ncomms7709
PMID:25833741

30. Shyer AE, Huycke TR, Lee C, Mahadevan L, Tabin CJ. Bending gradients: how the intestinal stem cell gets its home. Cell. 2015; 161:569–80.
https://doi.org/10.1016/j.cell.2015.03.041
PMID:25865482

31. Gerling M, Büller NV, Kirn LM, Joost S, Frings O, Englert B, Bergström Å, Kuiper RV, Blaas L, Wielenga MC, Almer S, Kühl AA, Fredlund E, et al. Stromal Hedgehog signalling is downregulated in colon cancer and its restoration restrains tumour growth. Nat Commun. 2016; 7:12321.
https://doi.org/10.1038/ncomms12321
PMID:27492255

32. Goetz SC, Bangs F, Barrington CL, Katsanis N, Anderson KV. The Meckel syndrome- associated

protein MKS1 functionally interacts with components of the BBSome and IFT complexes to mediate ciliary trafficking and hedgehog signaling. PLoS One. 2017; 12:e0173399.
https://doi.org/10.1371/journal.pone.0173399
PMID:28291807

33. Liem KF Jr, Ashe A, He M, Satir P, Moran J, Beier D, Wicking C, Anderson KV. The IFT-A complex regulates Shh signaling through cilia structure and membrane protein trafficking. J Cell Biol. 2012; 197:789–800.
https://doi.org/10.1083/jcb.201110049
PMID:22689656

34. Eguether T, Cordelieres FP, Pazour GJ. Intraflagellar transport is deeply integrated in hedgehog signaling. Mol Biol Cell. 2018; 29:1178–89.
https://doi.org/10.1091/mbc.E17-10-0600
PMID:29540531

35. Auerbach O, Stout AP. Histopathological aspects of occult cancer of the lung. Ann N Y Acad Sci. 1964; 114:803–10.
PMID:5220116

36. Gould PR, Li L, Henderson DW, Barter RA, Papadimitriou JM. Cilia and ciliogenesis in endometrial adenocarcinomas. An ultrastructural analysis. Arch Pathol Lab Med. 1986; 110:326–30.
PMID:3754121

37. Bao Z, Huang WJ. Thioridazine promotes primary ciliogenesis in lung cancer cells through enhancing cell autophagy. Int J Clin Exp Med. 2017; 10:13960–9.

38. Jung M, Häberle BM, Tschaikowsky T, Wittmann MT, Balta EA, Stadler VC, Zweier C, Dörfler A, Gloeckner CJ, Lie DC. Analysis of the expression pattern of the schizophrenia-risk and intellectual disability gene TCF4 in the developing and adult brain suggests a role in development and plasticity of cortical and hippocampal neurons. Mol Autism. 2018; 9:20.
https://doi.org/10.1186/s13229-018-0200-1
PMID:29588831

39. Murre C. Helix-loop-helix proteins and the advent of cellular diversity: 30 years of discovery. Genes Dev. 2019; 33:6–25.
https://doi.org/10.1101/gad.320663.118
PMID:30602438

40. Kennedy AJ, Rahn EJ, Paulukaitis BS, Savell KE, Kordasiewicz HB, Wang J, Lewis JW, Posey J, Strange SK, Guzman-Karlsson MC, Phillips SE, Decker K, Motley ST, et al. Tcf4 Regulates Synaptic Plasticity, DNA Methylation, and Memory Function. Cell Rep. 2016; 16:2666–85.
https://doi.org/10.1016/j.celrep.2016.08.004
PMID:27568567

41. Kaaij LT, van de Wetering M, Fang F, Decato B, Molaro A, van de Werken HJ, van Es JH, Schuijers J, de Wit E, de Laat W, Hannon GJ, Clevers HC, Smith AD, Ketting RF. DNA methylation dynamics during intestinal stem cell differentiation reveals enhancers driving gene expression in the villus. Genome Biol. 2013; 14:R50.
https://doi.org/10.1186/gb-2013-14-5-r50
PMID:23714178

42. Baratz KH, Tosakulwong N, Ryu E, Brown WL, Branham K, Chen W, Tran KD, Schmid-Kubista KE, Heckenlively JR, Swaroop A, Abecasis G, Bailey KR, Edwards AO. E2-2 protein and Fuchs's corneal dystrophy. N Engl J Med. 2010; 363:1016–24.
https://doi.org/10.1056/NEJMoa1007064
PMID:20825314

43. Amiel J, Rio M, de Pontual L, Redon R, Malan V, Boddaert N, Plouin P, Carter NP, Lyonnet S, Munnich A, Colleaux L. Mutations in TCF4, encoding a class I basic helix-loop-helix transcription factor, are responsible for Pitt-Hopkins syndrome, a severe epileptic encephalopathy associated with autonomic dysfunction. Am J Hum Genet. 2007; 80:988–93.
https://doi.org/10.1086/515582
PMID:17436254

44. Wray NR, Ripke S, Mattheisen M, Trzaskowski M, Byrne EM, Abdellaoui A, Adams MJ, Agerbo E, Air TM, Andlauer TMF, Bacanu SA, Bækvad-Hansen M, Beekman AFT, et al, and eQTLGen, and 23andMe, and Major Depressive Disorder Working Group of the Psychiatric Genomics Consortium. Genome-wide association analyses identify 44 risk variants and refine the genetic architecture of major depression. Nat Genet. 2018; 50:668–81.
https://doi.org/10.1038/s41588-018-0090-3
PMID:29700475

45. Ellinghaus D, Folseraas T, Holm K, Ellinghaus E, Melum E, Balschun T, Laerdahl JK, Shiryaev A, Gotthardt DN, Weismüller TJ, Schramm C, Wittig M, Bergquist A, et al. Genome-wide association analysis in primary sclerosing cholangitis and ulcerative colitis identifies risk loci at GPR35 and TCF4. Hepatology. 2013; 58:1074–83.
https://doi.org/10.1002/hep.25977
PMID:22821403

46. Kool M, Jones DT, Jäger N, Northcott PA, Pugh TJ, Hovestadt V, Piro RM, Esparza LA, Markant SL, Remke M, Milde T, Bourdeaut F, Ryzhova M, et al, and ICGC PedBrain Tumor Project. Genome sequencing of SHH medulloblastoma predicts genotype-related response to smoothened inhibition. Cancer Cell. 2014; 25:393–405.
https://doi.org/10.1016/j.ccr.2014.02.004
PMID:24651015

47. Hellwig M, Lauffer MC, Bockmayr M, Spohn M, Merk DJ, Harrison L, Ahlfeld J, Kitowski A, Neumann JE, Ohli J, Holdhof D, Niesen J, Schoof M, et al. TCF4 (E2-2) harbors tumor suppressive functions in SHH medulloblastoma. Acta Neuropathol. 2019; 137:657–73. https://doi.org/10.1007/s00401-019-01982-5 PMID:30830316

48. Gebert LFR, MacRae IJ. Regulation of microRNA function in animals. Nat Rev Mol Cell Biol. 2019; 20:21–37. https://doi.org/10.1038/s41580-018-0045-7 PMID:30108335

49. Graham RP, Nair AA, Davila JI, Jin L, Jen J, Sukov WR, Wu TT, Appelman HD, Torres-Mora J, Perry KD, Zhang L, Kloft-Nelson SM, Knudson RA, et al. Gastroblastoma harbors a recurrent somatic MALAT1-GLI1 fusion gene. Mod Pathol. 2017; 30:1443–52. https://doi.org/10.1038/modpathol.2017.68 PMID:28731043

50. Spans L, Fletcher CD, Antonescu CR, Rouquette A, Coindre JM, Sciot R, Debiec-Rychter M. Recurrent MALAT1-GLI1 oncogenic fusion and GLI1 up-regulation define a subset of plexiform fibromyxoma. J Pathol. 2016; 239:335–43. https://doi.org/10.1002/path.4730 PMID:27101025

51. Antonescu CR, Agaram NP, Sung YS, Zhang L, Swanson D, Dickson BC. A Distinct Malignant Epithelioid Neoplasm With GLI1 Gene Rearrangements, Frequent S100 Protein Expression, and Metastatic Potential: Expanding the Spectrum of Pathologic Entities With ACTB/MALAT1/PTCH1-GLI1 Fusions. Am J Surg Pathol. 2018; 42:553–60. https://doi.org/10.1097/PAS.0000000000001010 PMID:29309307

52. Prall OWJ, McEvoy CRE, Byrne DJ, Iravani A, Browning J, Choong DY, Yellapu B, O'Haire S, Smith K, Luen SJ, Mitchell PLR, Desai J, Fox SB, et al. A Malignant Neoplasm From the Jejunum With a *MALAT1-GLI1* Fusion and 26-Year Survival History. Int J Surg Pathol. 2020; 28:553–62. https://doi.org/10.1177/1066896919900548 PMID:31931637

53. Engreitz JM, Sirokman K, McDonel P, Shishkin AA, Surka C, Russell P, Grossman SR, Chow AY, Guttman M, Lander ES. RNA-RNA interactions enable specific targeting of noncoding RNAs to nascent Pre-mRNAs and chromatin sites. Cell. 2014; 159:188–99. https://doi.org/10.1016/j.cell.2014.08.018 PMID:25259926

54. West JA, Davis CP, Sunwoo H, Simon MD, Sadreyev RI, Wang PI, Tolstorukov MY, Kingston RE. The long noncoding RNAs NEAT1 and MALAT1 bind active chromatin sites. Mol Cell. 2014; 55:791–802. https://doi.org/10.1016/j.molcel.2014.07.012 PMID:25155612

55. Brandl L, Horst D, de Toni E, Kirchner T, Herbst A, Kolligs FT. ITF-2B protein levels are correlated with favorable prognosis in patients with colorectal carcinomas. Am J Cancer Res. 2015; 5:2241–8. PMID:26328254

56. Herbst A, Bommer GT, Kriegl L, Jung A, Behrens A, Csanadi E, Gerhard M, Bolz C, Riesenberg R, Zimmermann W, Dietmaier W, Wolf I, Brabletz T, et al. ITF-2 is disrupted via allelic loss of chromosome 18q21, and ITF-2B expression is lost at the adenoma-carcinoma transition. Gastroenterology. 2009; 137:639–48. https://doi.org/10.1053/j.gastro.2009.04.049 PMID:19394332

57. Grill JI, Herbst A, Brandl L, Kong L, Schneider MR, Kirchner T, Wolf E, Kolligs FT. Inactivation of Itf2 promotes intestinal tumorigenesis in Apc(Min/+) mice. Biochem Biophys Res Commun. 2015; 461:249–53. https://doi.org/10.1016/j.bbrc.2015.04.009 PMID:25869068

58. Malakar P, Shilo A, Mogilevsky A, Stein I, Pikarsky E, Nevo Y, Benyamini H, Elgavish S, Zong X, Prasanth KV, Karni R. Long Noncoding RNA MALAT1 Promotes Hepatocellular Carcinoma Development by SRSF1 Upregulation and mTOR Activation. Cancer Res. 2017; 77:1155–67. https://doi.org/10.1158/0008-5472.CAN-16-1508 PMID:27993818

59. Ji Q, Zhang L, Liu X, Zhou L, Wang W, Han Z, Sui H, Tang Y, Wang Y, Liu N, Ren J, Hou F, Li Q. Long non-coding RNA MALAT1 promotes tumour growth and metastasis in colorectal cancer through binding to SFPQ and releasing oncogene PTBP2 from SFPQ/PTBP2 complex. Br J Cancer. 2014; 111:736–48. https://doi.org/10.1038/bjc.2014.383 PMID:25025966

60. Kim J, Piao HL, Kim BJ, Yao F, Han Z, Wang Y, Xiao Z, Siverly AN, Lawhon SE, Ton BN, Lee H, Zhou Z, Gan B, et al. Long noncoding RNA MALAT1 suppresses breast cancer metastasis. Nat Genet. 2018; 50:1705–15. https://doi.org/10.1038/s41588-018-0252-3 PMID:30349115

61. Han Y, Wu Z, Wu T, Huang Y, Cheng Z, Li X, Sun T, Xie X, Zhou Y, Du Z. Tumor-suppressive function of long noncoding RNA MALAT1 in glioma cells by downregulation of MMP2 and inactivation of ERK/MAPK signaling. Cell Death Dis. 2016; 7:e2123. https://doi.org/10.1038/cddis.2015.407 PMID:26938295

62. Conlon K, Watson DC, Waldmann TA, Valentin A, Bergamaschi C, Felber BK, Peer CJ, Figg WD, Potter EL, Roederer M, McNeel DG, Thompson JA, Gupta S, et al. Phase I study of single agent NIZ985, a recombinant heterodimeric IL-15 agonist, in adult patients with metastatic or unresectable solid tumors. J Immunother Cancer. 2021; 9:e003388. https://doi.org/10.1136/jitc-2021-003388 PMID:34799399

63. Gilad Y, Gellerman G, Lonard DM, O'Malley BW. Drug Combination in Cancer Treatment-From Cocktails to Conjugated Combinations. Cancers (Basel). 2021; 13:669. https://doi.org/10.3390/cancers13040669 PMID:33562300

64. Bhatia K, Bhumika, Das A. Combinatorial drug therapy in cancer - New insights. Life Sci. 2020; 258:118134. https://doi.org/10.1016/j.lfs.2020.118134 PMID:32717272

65. Nagy Á, Munkácsy G, Győrffy B. Pancancer survival analysis of cancer hallmark genes. Sci Rep. 2021; 11:6047. https://doi.org/10.1038/s41598-021-84787-5 PMID:33723286

66. Tang Z, Kang B, Li C, Chen T, Zhang Z. GEPIA2: an enhanced web server for large-scale expression profiling and interactive analysis. Nucleic Acids Res. 2019; 47:W556–60. https://doi.org/10.1093/nar/gkz430 PMID:31114875

67. Huang da W, Sherman BT, Lempicki RA. Systematic and integrative analysis of large gene lists using DAVID bioinformatics resources. Nat Protoc. 2009; 4:44–57. https://doi.org/10.1038/nprot.2008.211 PMID:19131956

68. Szklarczyk D, Gable AL, Lyon D, Junge A, Wyder S, Huerta-Cepas J, Simonovic M, Doncheva NT, Morris JH, Bork P, Jensen LJ, Mering CV. STRING v11: protein-protein association networks with increased coverage, supporting functional discovery in genome-wide experimental datasets. Nucleic Acids Res. 2019; 47:D607–13. https://doi.org/10.1093/nar/gky1131 PMID:30476243

69. Shannon P, Markiel A, Ozier O, Baliga NS, Wang JT, Ramage D, Amin N, Schwikowski B, Ideker T. Cytoscape: a software environment for integrated models of biomolecular interaction networks. Genome Res. 2003; 13:2498–504. https://doi.org/10.1101/gr.1239303 PMID:14597658

70. Li LC, Dahiya R. MethPrimer: designing primers for methylation PCRs. Bioinformatics. 2002; 18:1427–31. https://doi.org/10.1093/bioinformatics/18.11.1427 PMID:12424112

71. Hu H, Miao YR, Jia LH, Yu QY, Zhang Q, Guo AY. AnimalTFDB 3.0: a comprehensive resource for annotation and prediction of animal transcription factors. Nucleic Acids Res. 2019; 47:D33–8. https://doi.org/10.1093/nar/gky822 PMID:30204897

72. Castro-Mondragon JA, Riudavets-Puig R, Rauluseviciute I, Lemma RB, Turchi L, Blanc-Mathieu R, Lucas J, Boddie P, Khan A, Manosalva Pérez N, Fornes O, Leung TY, Aguirre A, et al. JASPAR 2022: the 9th release of the open-access database of transcription factor binding profiles. Nucleic Acids Res. 2022; 50:D165–73. https://doi.org/10.1093/nar/gkab1113 PMID:34850907

73. Huang HY, Li J, Tang Y, Huang YX, Chen YG, Xie YY, Zhou ZY, Chen XY, Ding SY, Luo MF, Jin CN, Zhao LS, Xu JT, et al. MethHC 2.0: information repository of DNA methylation and gene expression in human cancer. Nucleic Acids Res. 2021; 49:D1268–75. https://doi.org/10.1093/nar/gkaa1104 PMID:33270889

74. Chen F, Chandrashekar DS, Varambally S, Creighton CJ. Pan-cancer molecular subtypes revealed by mass-spectrometry-based proteomic characterization of more than 500 human cancers. Nat Commun. 2019; 10:5679. https://doi.org/10.1038/s41467-019-13528-0 PMID:31831737

75. Karagkouni D, Paraskevopoulou MD, Tastsoglou S, Skoufos G, Karavangeli A, Pierros V, Zacharopoulou E, Hatzigeorgiou AG. DIANA-LncBase v3: indexing experimentally supported miRNA targets on non-coding transcripts. Nucleic Acids Res. 2020; 48:D101–10. https://doi.org/10.1093/nar/gkz1036 PMID:31732741

76. Li JH, Liu S, Zhou H, Qu LH, Yang JH. starBase v2.0: decoding miRNA-ceRNA, miRNA-ncRNA and protein-RNA interaction networks from large-scale CLIP-Seq data. Nucleic Acids Res. 2014; 42:D92–7. https://doi.org/10.1093/nar/gkt1248 PMID:24297251

77. Li T, Fu J, Zeng Z, Cohen D, Li J, Chen Q, Li B, Liu XS. TIMER2.0 for analysis of tumor-infiltrating immune cells. Nucleic Acids Res. 2020; 48:W509–14. https://doi.org/10.1093/nar/gkaa407 PMID:32442275

78. Cerami E, Gao J, Dogrusoz U, Gross BE, Sumer SO, Aksoy BA, Jacobsen A, Byrne CJ, Heuer ML, Larsson E, Antipin Y, Reva B, Goldberg AP, et al. The cBio cancer

genomics portal: an open platform for exploring multidimensional cancer genomics data. Cancer Discov. 2012; 2:401–4.
https://doi.org/10.1158/2159-8290.CD-12-0095
PMID:22588877

79. Gao J, Aksoy BA, Dogrusoz U, Dresdner G, Gross B, Sumer SO, Sun Y, Jacobsen A, Sinha R, Larsson E, Cerami E, Sander C, Schultz N. Integrative analysis of complex cancer genomics and clinical profiles using the cBioPortal. Sci Signal. 2013; 6:pl1.
https://doi.org/10.1126/scisignal.2004088
PMID:23550210

80. Jiang W, Qu Y, Yang Q, Ma X, Meng Q, Xu J, Liu X, Wang S. D-lnc: a comprehensive database and analytical platform to dissect the modification of drugs on lncRNA expression. RNA Biol. 2019; 16:1586–91.
https://doi.org/10.1080/15476286.2019.1649584
PMID:31390943

81. Liu E, Liu Z, Zhou Y. Carboplatin-docetaxel-induced activity against ovarian cancer is dependent on up-regulated lncRNA PVT1. Int J Clin Exp Pathol. 2015; 8:3803–10.
PMID:26097562

82. Pan F, Zhu L, Lv H, Pei C. Quercetin promotes the apoptosis of fibroblast-like synoviocytes in rheumatoid arthritis by upregulating lncRNA MALAT1. Int J Mol Med. 2016; 38:1507–14.
https://doi.org/10.3892/ijmm.2016.2755
PMID:28026003

SUPPLEMENTARY MATERIALS

Supplementary Figures

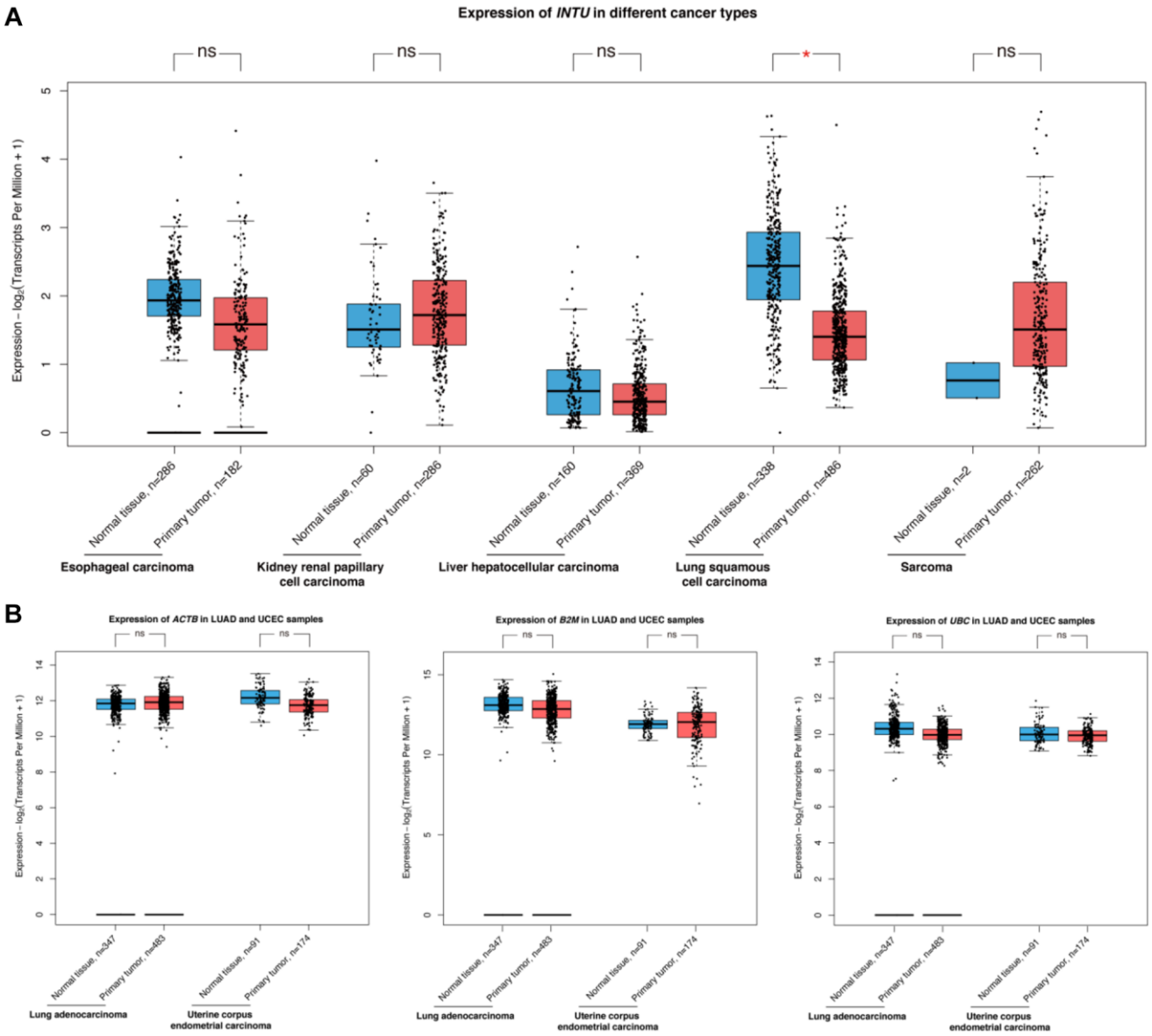

Supplementary Figure 1. Evaluation of *INTU* and housekeeping gene levels in different cancer types. (**A**) The expression of *INTU* was significantly downregulated in LUSC tumor samples. The *INTU* expression was not significantly altered in ESCA, KIRP, LIHC and SARC tumor samples when compared to their respective normal control samples. (**B**) The expression of housekeeping genes *ACTB*, *B2M* and *UBC* was not altered in LUAD and UCEC tumor samples when compared to their respective normal control samples.

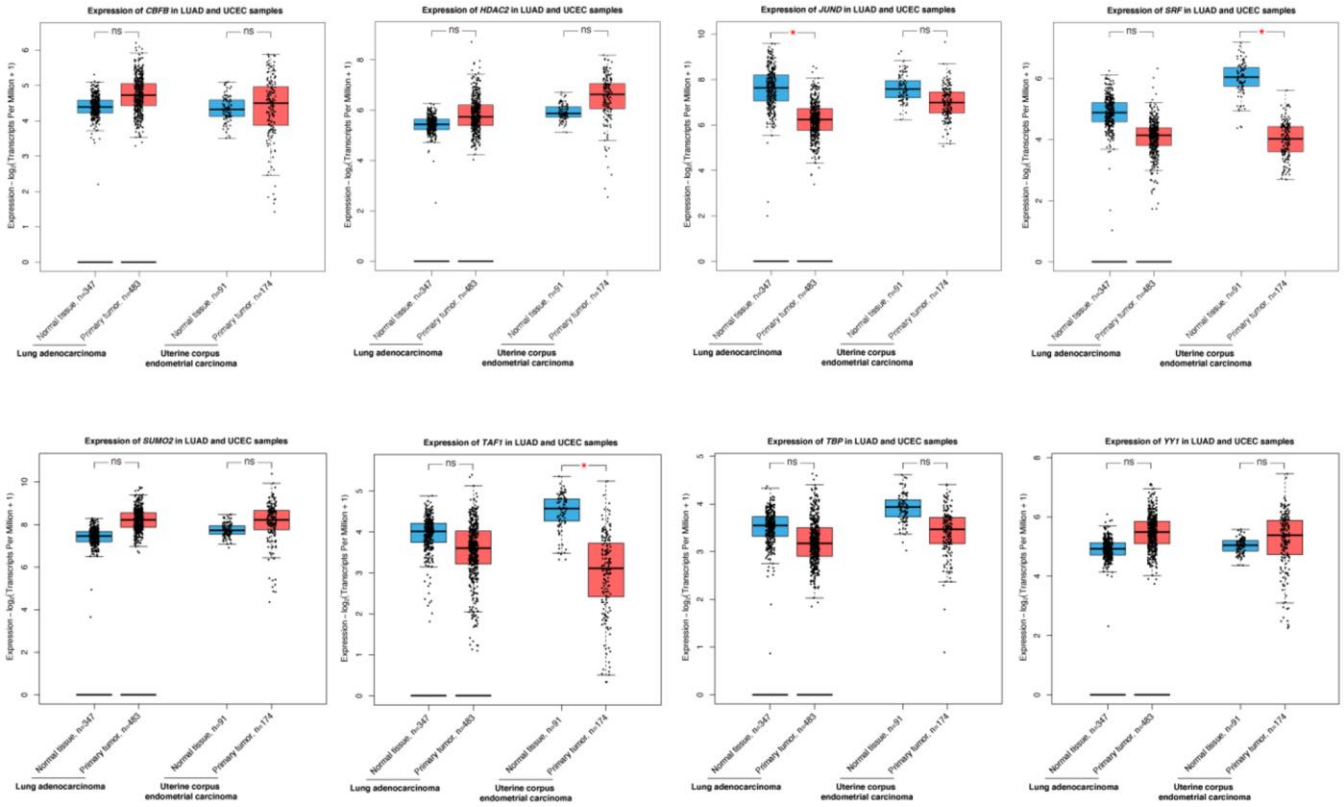

Supplementary Figure 2. Examination of *CBFB*, *HDAC2*, *JUND*, *SRF*, *SUMO2*, *TAF1*, *TBP* and *YY1* levels in LUAD and UCEC samples. None of the transcription factors examined showed significant change of expression in both LUAD and UCEC tumor samples.

Supplementary Figure 3. Evaluation of the correlation between *hsa-miR-210-3p* expression and *INTU* and *IFT88* levels in LUAD and UCEC tumor samples. No significant correlation was detected between the expression of *hsa-miR-210-3p* and mRNA levels of *INTU* and *IFT88* in LUAD and UCEC tumor samples, except for in LUAD tumor samples, expression of *hsa-miR-210-3p* negatively correlated with *IFT88* mRNA level.

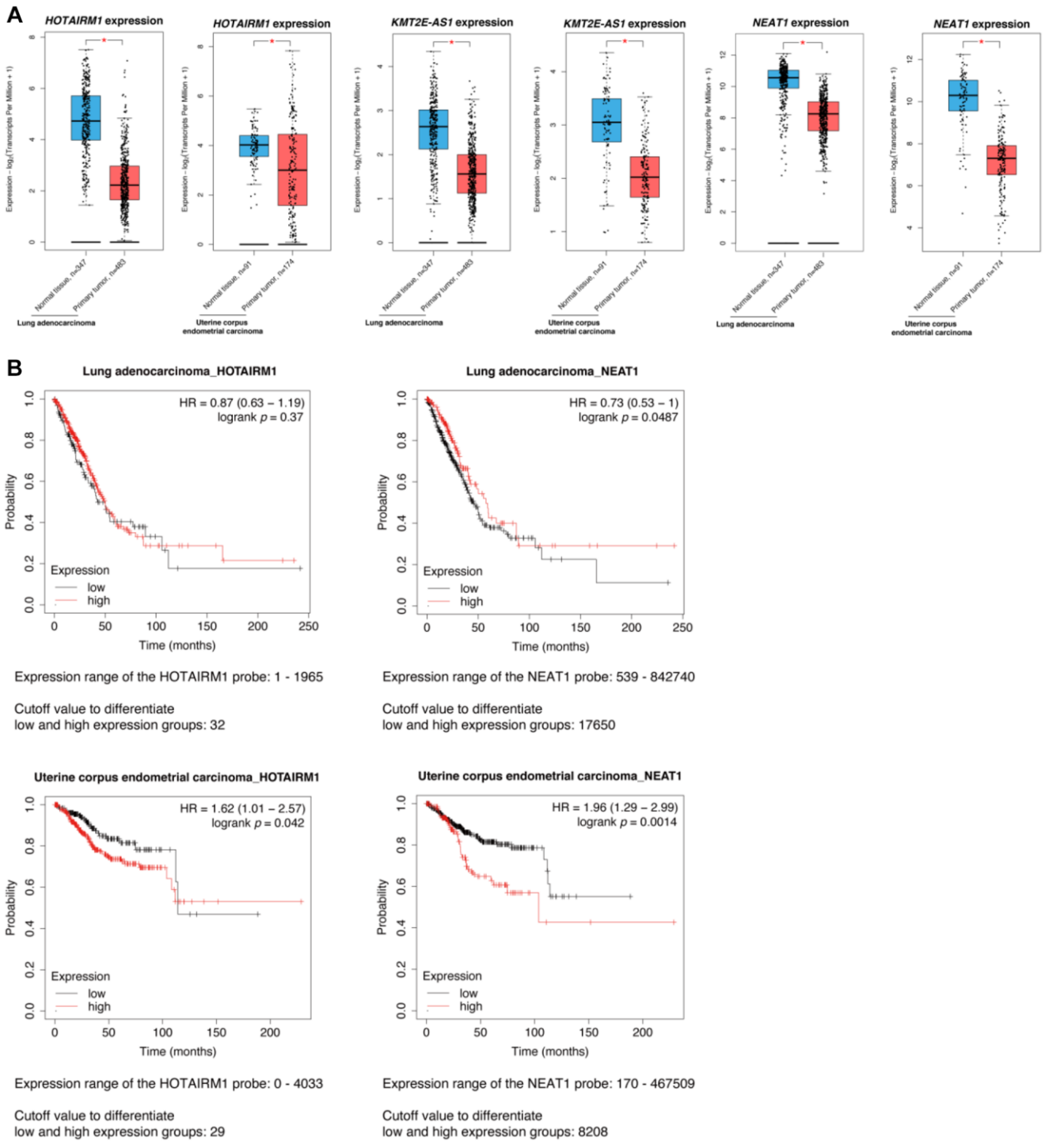

Supplementary Figure 4. Evaluation of the expression and prognostic significance of lncRNAs in LUAD and UCEC tumor samples. (**A**) The expression of *HOTAIRM1*, *KMT2E-AS1* and *NEAT1* was significantly downregulated in LUAD and UCEC tumor samples. (**B**) The LUAD patients with decreased *NEAT1* level showed reduced survival probabilities. Higher levels of *HOTAIRM1* and *NEAT1* were found associated with poor survival probabilities in UCEC patients. No correlation between *HOTAIRM1* level and OS probabilities was detected in LUAD patients.

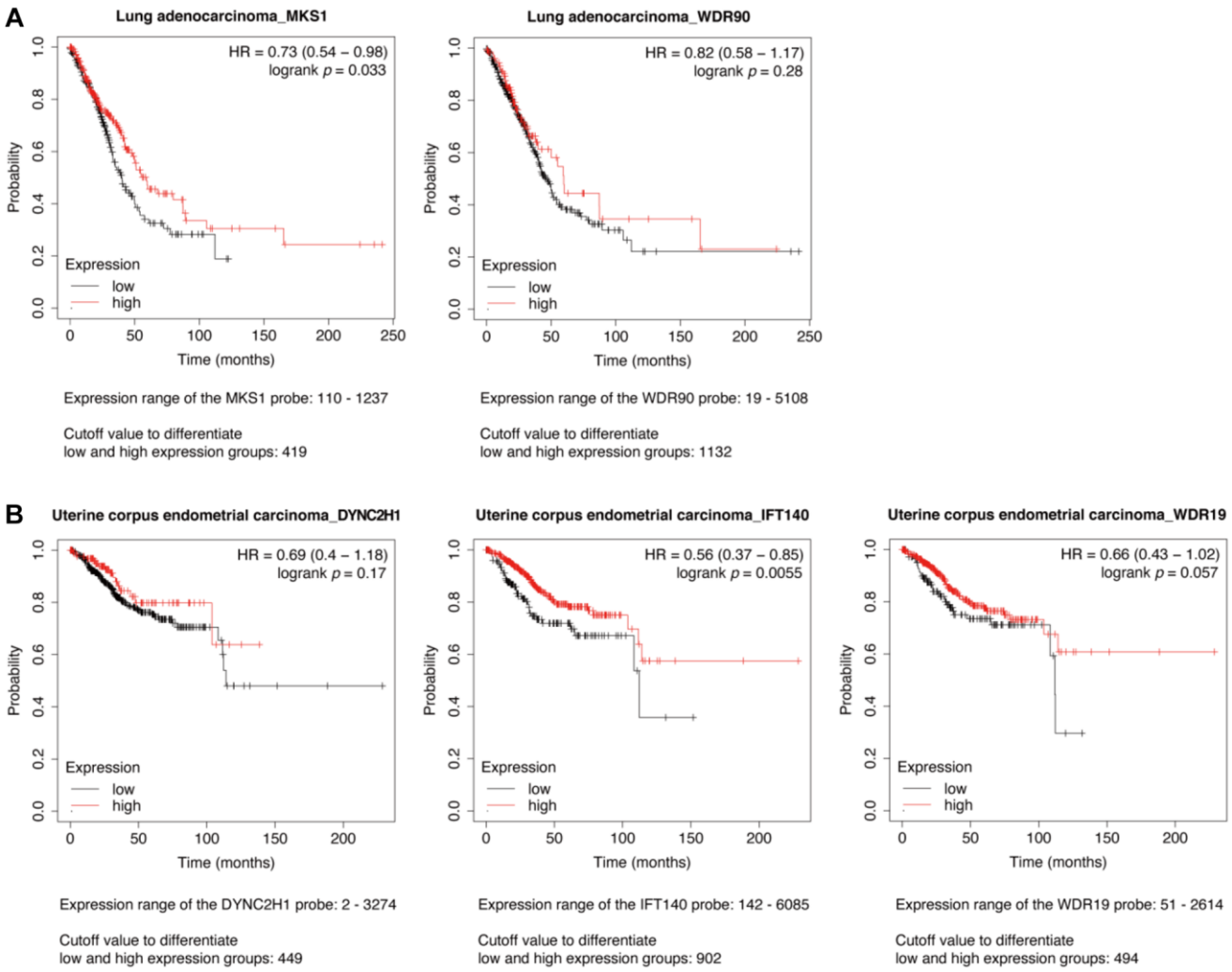

Supplementary Figure 5. Evaluation of the prognostic significance of enriched Hh-related genes in LUAD and UCEC patients. (**A**) Decreased level of *MKS1* correlated with poor OS probabilities in LUAD patients, whilst the *WDR90* level didn't show a significant correlation with OS probabilities in LUAD patients. (**B**) The UCEC patients with lowered *IFT140* level showed decreased OS probabilities. Neither *DYNC2H1* nor *WDR19* level significantly correlated with OS probabilities in UCEC patients.

A

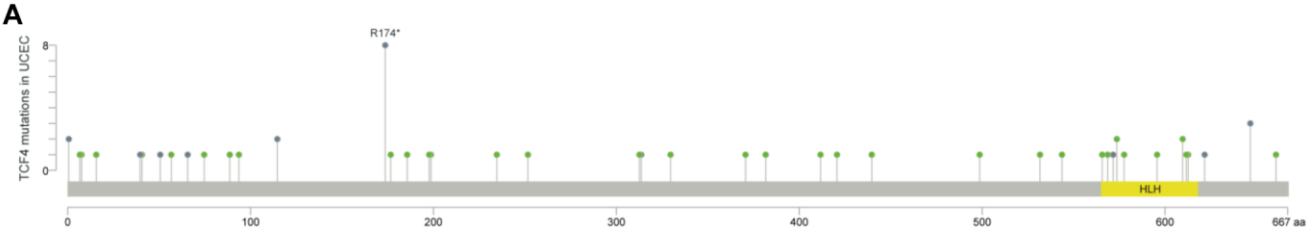

B

Cancer type	Sample ID	TCF4 mutation			Functional Impacts	
		Amino acid change	HGVSc	Mutation type	SIFT	MutationAssessor
Uterine Corpus Endometrial Carcinoma	TCGA-AP-A056-01	R174*	ENST00000356073.4:c.520C>T	Nonsense	N/A	N/A
Uterine Corpus Endometrial Carcinoma	TCGA-AX-A05Z-01					
Uterine Corpus Endometrial Carcinoma	TCGA-B5-A0JY-01					
Uterine Corpus Endometrial Carcinoma	TCGA-B5-A11E-01					
Uterine Corpus Endometrial Carcinoma	TCGA-B5-A1MR-01					
Uterine Corpus Endometrial Carcinoma	TCGA-BS-A0UF-01					
Uterine Corpus Endometrial Carcinoma	TCGA-EO-A3AV-01					
Uterine Corpus Endometrial Carcinoma	TCGA-QF-A5YS-01					

C

Supplementary Figure 6. Illustration of the mutations in TCF4 protein from LUAD and UCEC tumor samples. (**A**) A relative higher mutation frequency was identified at TCF4^{R174} residue from UCEC tumor samples. (**B**) The detailed mutation site of TCF4^{R174} mutant protein from UCEC tumor samples. (**C**) The TCF4^{R174} residue was highly conserved among different species.

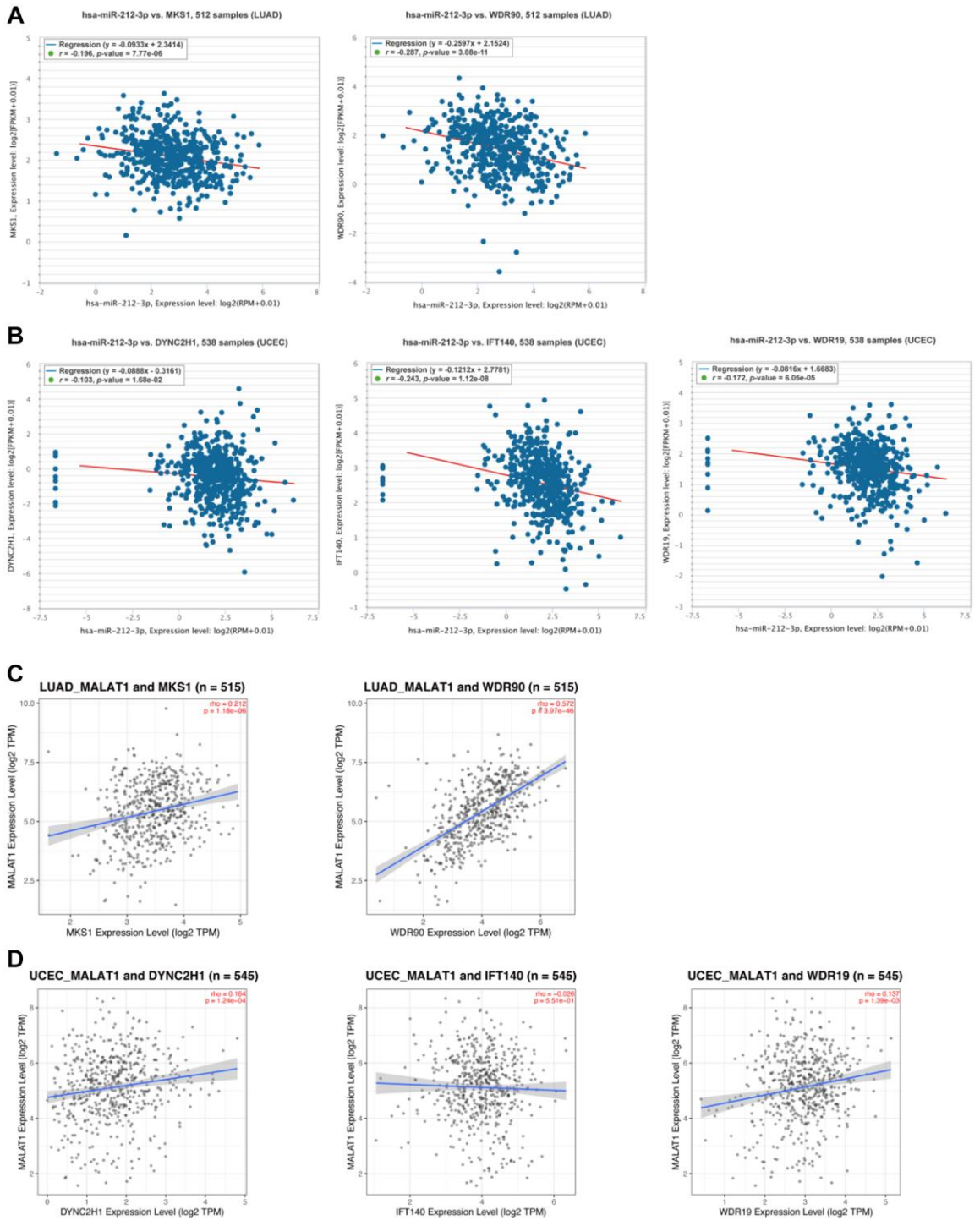

Supplementary Figure 7. The *MALAT1-hsa-miR-212-3p* signaling axis regulates enriched Hh-related genes in LUAD and UCEC samples. (**A**) The expression of *hsa-miR-212-3p* was found negatively associated with the mRNA levels of *MKS1* and *WDR90* in LUAD samples. (**B**) Negative correlation was determined between *hsa-miR-212-3p* expression and mRNA levels of *DYNC2H1*, *IFT140* and *WDR19* in UCEC samples. (**C**) The expression of *MALAT1* positively correlated with the levels of *MKS1* and *WDR90* in LUAD samples. (**D**) The expression of *MALAT1* positively correlated with the levels of *DYNC2H1* and *WDR19* in UCEC samples. No significant correlation was determined between *MALAT1* and *IFT140*.

Supplementary Tables

Please browse Full Text version to see the data of Supplementary Table 1.

Supplementary Table 1. The top 100 genes with similar expression patterns as *INTU* from LUAD and UCEC tumor samples.

Supplementary Table 2. The promoter sequences of *INTU* and *IFT88*.

***INTU* gene promoter sequence (*INTU*^{CpG} sequence is in blue and TCF4 binding site is highlighted):**
ATCATTAATCTGTAATCTATAACCTATGATAGCTCACATTTTAAACTATTACGCTCCAGTTTCTCCATTTATTCTCC TTCAGTGGTTCCCCTTACCATTCTGGCCTGTTCTGACTTAGGGACAGTCTACAGTAGGAAGTCACACACGCGTCA CTTTTCCCACGATGGAAAAACCACCAAGCTAATTTTGTCTTCTCTTTGACCACAGGCCATAGAATAGTTCACTGA AATACCTAATGCCCTAGAGTAGAGACTGTCTCCTGGGGTCAAGTATATTTTAAAGCAAATAAATCCCCCCAAAA GAGAATAAAGCCACATTAGACAAGTCAGAGTCCACCTTTTATTCACTCTTGTACCTCCAAGGACTAGAACTCGGC CTGGCACATAGCAAGTGGTAATACACATTTGCACGGACGGATGAATGTATATGGCTTCTTTAGGCTGAATTAAA ACTCCCACCAAGAGCAGACAACTACCTTGCCTCTTCCCCACTCGTTTTCGGGTCTTCCACAGAGCAGCCAGAGCC TCAGAGGCCCTTGAGAGTTTCCTCCACTCCTCCCTTGTTTGCAGCGCTAGAAGCTGCAGGTGGTAGTTCCTACAC TGGGGGCGGCGCCTGGACGCGGGTGTCCCTGGCCAAGGCGGCCTCGCTGTCCTGGAAGGGAGGGTGAAGAGCT GCATCCCGCACTAGGCGGCGAAAGAGGGCAGCGCCAAGCGGCGGGGTCCGGAGGCGCTCGACGGCTCGCGCCC AGCGCCGGAGACGGGCTGTGTGTTGGGCCAGTGGAAGACACCGGAGAAACCCAGACGTGGAAGACCGGGCAGC CTGGACTTCGCGAGCCCTGGTGGGGCTGGCGGCCCACAGAGCCCCCACCTGCCCCGAGCTCCCACAGCGAGGAG TGGCCGCGCCGCCCGCCAGTGCGCCGGGCTCCGAGACCGGCAGGGGAGCACGCGGGCGAAGGAGGGGCCGCCG TCGCTGACACCACCGCCTTCAGCCCTTGGCTTCCGCGCGTCGGAGGCTGGCACCTCCAGGTTCACCGCGGCGGCC GGAGCTGTGCGGGGGCCAGACGGTTCGGCGGGAGCCGGGGCTGGGACCTGGGTGACCTGTCGTCCGCCCCTGTA GCGAGTCTCCAGTGGGCATGTTTCAGGTGGGCAGGTCCAGCATCCCCAAACCTGCCCCCCGCAGCCTGGAGGAC CTGGACTCAGTGCAGCGTGTCCTGTTACACAG.
***IFT88* gene promoter sequence (*IFT88*^{CpG} sequence is in blue and TCF4 binding site is highlighted):**
GCTGGTCTCCAACTCCTCACCTCAGGTGATCCGCCAGCCTCAGCCTCCCAAAGTGCTGGGATTATAGGCATGAGC CACTGCGCCCGGCCAACACTACTTATTTTATAAAAACTCATTAATTACTGGTGTCTTTAGACTCCCTCTGTCCCTC CCCTCCATCCCCAACATTTACTTTTAAAATTTAAGACAAAACTTAAACATTAAACAATTATGAATTTAATTCCCCC ATTTATATTACATTGATTAAGCTTTACACTATGACCCAGGTTCTAGGTGGTTGGGACACAATGGTTCAATCCCTGT CTAGTAAATAAAACGGACACCTTAAGCGCTACAATCAAGGTGCGCACGGGGTGCTACAGAACAATACGCAGAC AGGAGGAGGTGGGGGGAAAGGTGAGACTTCCCAGGCAGGTGTCATCCCAGAATAACTTTTACACAGGGTGACT AAGCGAGTTAGTGACTGCGCGGAAAACGGGCTTCCAAGGTTCACAAGGCTCGTGCTGCGGCTCCGGGAGTTATG TCACAGTAAGCTTACTATCATCCTTTGGGCATCTGCTTTACGGATGAGTTCATCAGGATTTAAAGGATCTTGGTTC CATATCCTTCCCCTTCCTCACAGAGGCCGCCAGCCCGGAGCCCCTCTAGGCCCTCCTCCCTCCTGCATCTACTGGC CGCGAGCCTTTCCCTCCCCGCCCCCTTCACACAGGCCGCCCCCAGCCTCCCAACCCCCCGGTTCCGTTCCACGGG AGGCCCCGGCCTCCCTGCCCTCTCCTCCACCGTTCTACCCGCATCGCCCGGCTTCCCGCAAGCCGCTGGCACCGT CCCCTCAACACCCTCCGCCCACCGCCACTCCCTTCCACTGAGGGGGACCGGGCTGCCTTCTCTCTGACCCGCCGT TCTCCGCCCCCACCCACTTCCCCAGGCCTCCCGCACCACCCCCTTCCCGCCGCGCTCTCTCCCGCCCCCGCGCTTC CGGCCCCGCCCGCCCCCGCGCGGAGGACTGTGGGAGCGGCTTCCTTGGATTCCGCGCTTGGCAACGGCTCGGCG TCGCGCTTTGGCCAACCGCTGCGTCGTCCCTGGGCCCGAATAACTGTCGCCCGCTTCCCTCAGCGTGAG.